British Geological Survey

DFID Department For International Development

TECHNICAL REPORT WC/97/59
Overseas Geology Series

ELECTROKINETIC SOUNDING APPLIED TO WELL AND BOREHOLE SITING: AN APPRAISAL

D Beamish and R J Peart

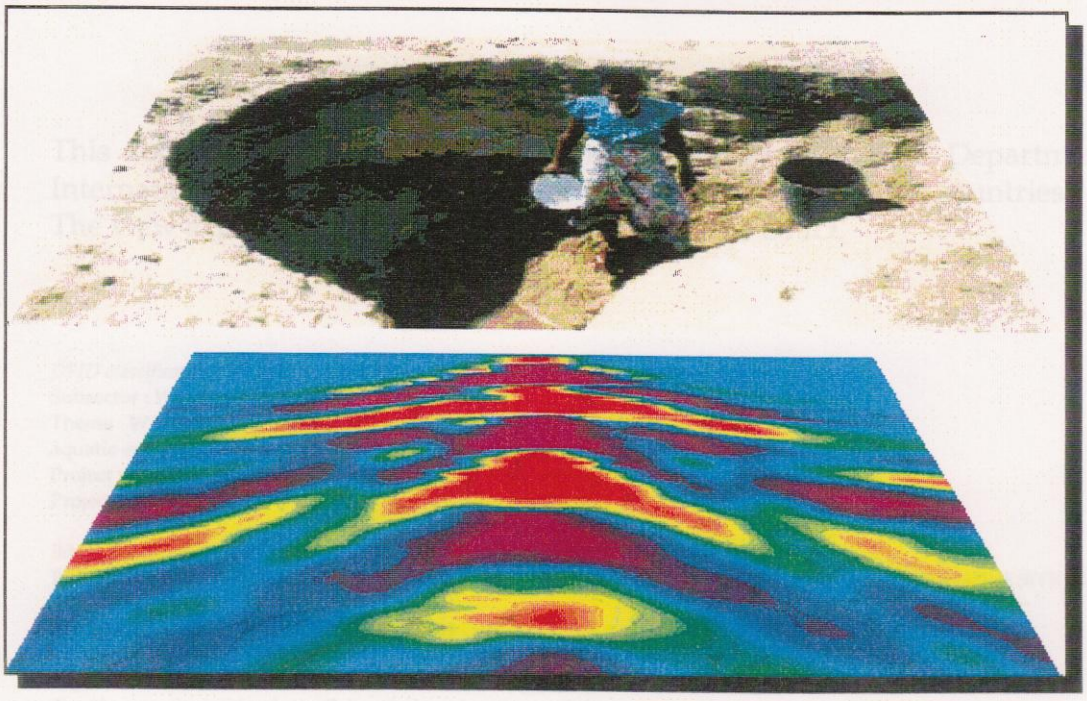

Natural Environment Research Council

International Division
British Geological Survey
Keyworth
Nottingham NG12 5GG
United Kingdom

DFID Department For International Development

British Geological Survey

TECHNICAL REPORT WC/97/59
Overseas Geology Series

ELECTROKINETIC SOUNDING APPLIED TO WELL AND BOREHOLE SITING: AN APPRAISAL

D Beamish and R J Peart

This document is an output from a project funded by the UK Department for International Development (DFID) for the benefit of developing countries. The view expressed are not necessarily those of the DFID.

DFID classification :
Subsector : Water and Sanitation
Theme : W2- Increase protection of water resources, water quality and aquatic ecosystems
Project title : Development of new well siting techniques
Project reference : R6232

Bibliographic reference :
Beamish D and Peart, R J, 1997. ELECTROKINETIC SOUNDING APPLIED TO WELL AND BOREHOLE SITING: AN APPRAISAL
British Geological Survey Report WC/97/59

Keywords :
Geophysics, electrokinetic, well, borehole, siting, permeability

Front cover illustration :
Perspective views of water-hole and acoustic moveout experiments in Zimbabwe..

Keyworth, Nottingham, British Geological Survey, 1997

CONTENTS

		Page
1.	**INTRODUCTION**	**1**
2.	**SCOPE OF THE REPORT**	**1**
3.	**HISTORICAL BACKGROUND**	**2**
4.	**THEORY**	**3**
4.1	Porous rocks and streaming potential	3
4.2	The acoustic source	4
4.3	The vertical electric dipole	6
4.4	Predictions from theory	7
5.	**TWO-CHANNEL EK SOUNDING**	**9**
5.1	Estimation of porosity/permeability	11
5.2	Field experiments overseas	12
5.3	Field experiments in the UK	13
6.	**MULTI-CHANNEL EK SOUNDING**	**16**
6.1	Case study 1. Sherwood Sandstone	17
6.2	Case study 2. Sherwood Sandstone	17
6.3	Case study 3. Gore sand river, Zimbabwe	19
6.4	Case study 4. Dartmoor granite	19
7.	**SUMMARY**	**21**
8.	**THE WAY FORWARD**	**23**
9.	**REFERENCES**	**24**
10.	**ACKNOWLEDGEMENTS**	**25**

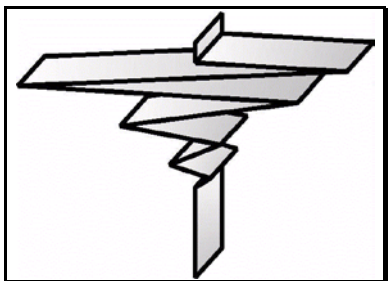

List of Figures

Figure 4.1 Schematic representation of the electrical double layer at a pore wall.

Figure 4.2 Schematic of the potential distribution across the electrical double layer.

Figure 4.3 Radius of first Fresnel zone. Variation with depth in 4 materials from low to high acoustic velocity.

Figure 4.4 Theoretical Ricker wavelets. Frequencies of 500, 200 and 100 Hz.

Figure 4.5 Schematic of the relative positions of various type of compressional seismic waves.

Figure 4.6 Subsurface cross-section showing contours of the horizontal electric field due to a vertical electric dipole.

Figure 4.7 Variation of amplitude of horizontal electric field generated by a buried vertical dipole at depths from 1 to 50 m.

Figure 4.8 Results of synthetic EK modelling from Mikhailov et al. (1997).

Figure 5.1 Illustration of electrokinetic data acquisition and processing sequence.

Figure 5.2 Example of EKS data repeatability.

Figure 5.3 Overlay of 7 EK soundings along a sand river profile.

Figure 5.4 Typical shot-symmetric, two-channel sounding curves above a sandstone aquifer.

Figure 5.5 2-channel EK sounding curves. Hall Farm test site borehole.

Figure 5.6 A comparison of field hydraulic conductivity results from in-situ hydraulic testing and EK sounding. Hall Farm, East Anglia.

Figure 5.7 2-channel EK sounding curves. Two sets of adjacent (5 m) soundings. Typical clay response.

Figure 5.8 Colour-contoured EK voltage data along a profile.

Figure 6.1 Schematic of acoustic and electrokinetic waves generated at a single interface.

Figure 6.2 True voltage amplitudes for dipole lengths from 1 to 10 m, using same inner dipole at 0.5 m.

Figure 6.3 Moveout experiment CoxM-N07.

Figure 6.4 Colour-contoured time/distance sections of voltage data. Profile CoxM.

Figure 6.5 Three soundings, same location, made with 3 electrode types.

Figure 6.6 Moveout experiment ClumbP-N15.

Figure 6.7 Colour-contoured time/distance section of voltage data. Profile ClumbP-N15.

Figure 6.8 Colour-contoured time/distance section of acoustic data. Profile ClumbP-N15.

Figure 6.9 Maximum entropy power spectra of EK soundings.

Figure 6.10 Maximum entropy power spectra of acoustic data.

Figure 6.11 Detailed joint moveout experiment from the Gore sand river in southern Zimbabwe.

Figure 6.12 EK soundings at 25 m along profile. Postbridge survey, Dartmoor granite.

Figure 6.13 EK soundings at 70 m along profile. Postbridge survey, Dartmoor granite.

Figure 6.14 Colour-contoured EK voltage data along profile. Postbridge survey. 0-100 ms.

Figure 6.15 Colour-contoured EK voltage data along profile. Postbridge survey. 100-200 ms.

1) INTRODUCTION

his report is written to summarise the findings of project R6232 whose goal was to improve the assessment, development and management of water resources. The stated purpose was 'to increase the success rate of well and borehole siting, in diverse hydrogeological environments, by assessing and developing a 'new' electrokinetic (EK) geophysical methodology'. With hindsight, the assessment and development requirements have proved to be far more intricate and involved than was originally envisaged. Simple hydrogeological questions (does the method work, or have any value?) have, of necessity, required detailed geophysical research.

One of the reasons for the complexity stems from the technical platform used for the assessments. The EK instrument and procedures were purchased from a new company who had developed the world's first commercial system for EK sounding. The claims made for the system were considerable; the available background to the methodology was minimal. In order to provide objectivity, it has been necessary to review and examine the physical theory alongside the measurement/processing techniques used. These developments had then to be assessed alongside the results of field experiments both in the UK and overseas.

A second reason for the complexity has been the nature of the wavefields employed The two fields used are acoustic (source) and electromagnetic (received). Individually both fields are well-defined following established geophysical methodologies which routinely employ them. The EK method exploits subsurface *coupling* of these wavefields. Theoretical predictions concerning the nature of the fully-coupled wavefields are difficult and limited. To our knowledge there is only one recent paper (Mikhailov et al.,1997) that attempts to deal adequately and practically with the numerical simulation of electrokinetic signals observed in the field. Even this assessment is quite limited.

Given that the EK methodology is new and the theoretical tools for prediction and modelling are limited, it is inevitable that a level of controversy will exist as the science progresses. Typically it is anticipated that simplifying assumptions will be made, observations/theory will test the assumptions and refinements will be made. At the outset it is worth stating that we acknowledge that subsurface EK coupling is routinely observed, however it is the interpretation of such data that has been a key issue in the project.

2) SCOPE OF THE REPORT

This report is intended to be reasonably self-contained. Following a brief historical background, the theoretical concepts underpinning electrokinetics are discussed in terms of (i) porous rocks and streaming potentials, (ii) the acoustic source and (iii) the vertical electric dipole. These concepts are then extended to consider the predictions that the limited theory, available to us at the present time, allows.

The commercial EK instrument and procedures employed initially in the Project conform to a special case, referred to here as two channel EK sounding. The principles and simplifying assumptions are discussed in some detail with extracts from the user manual. Overseas experiments involving two channel operation have been extensively described in previous technical reports (Beamish et al., 1977; Peart et al., 1995; Peart et al., 1997a,b); only a resume of this work is provided here. Although many UK experiments have been carried out, only three case studies which provide important diagnostic information are discussed.

During the latter half of the project, increasing use was made of multi-channel methods to provide a more complete description of the temporal/spatial nature of the voltages generated. Each electrokinetic ‘moveout’ experiment was performed in conjunction with a corresponding acoustic experiment. Although the theoretical concepts do not necessarily predict a simple correspondence between voltage (EK signal) and acoustic recordings, the seismic wave is the source of EK coupling and its behaviour must be addressed. In addition to these experiments, larger scale (i.e. spread lengths of 50 to 100 m) seismic refraction experiments were carried out to investigate the shallow velocity structure at each location. These experiments were conducted with an ABEM Terraloc seismic acquisition system. Four case studies, from the UK and overseas, which define the extended behaviour of EK voltages in a variety of diverse hydrogeological environments are discussed.

The final two sections of the report cover first a summary of the main findings and secondly a series of statements considering the way forward. This latter section also briefly considers other hydrogeophysical methodologies. Since the report is, in part, technically complex important summarising statements are included as text boxes to highlight some of the main points.

3) HISTORICAL BACKGROUND

The idea that sound waves could generate electric fields was discussed in a paper in the first volume of the Journal of Chemical Physics by Debye (1933) in connection with a suspension of charged particles forming an electrolytic solution. Such 'electro-acoustic' techniques, applied to the determination of the electrokinetic potential (at ultrasound frequencies), have become traditional tools for the industrial/laboratory characterisation of colloids and emulsions (O'Brien, 1988).

In the first volume of the journal Geophysics, Thompson (1936) proposed that the coupling of seismic and electric fields could be used as an exploration tool. The concept discussed was the variation in resistivity with elastic deformation and the term seismic electric effect was coined.

Ivanov (1939) made observations of electric fields generated by explosions. It was noted that there was a phase reversal in the electric field recorded when the elastic wave was generated on opposite sides of the electrode spread. The effect observed was discussed in terms of the solid and liquid phases present in the rock mass. Electrokinetic phenomena were described in terms of charge separation at the 'double diffusion layer' of the pore space. The same studies and concepts as those presented by Ivanov (1939) are now being reinvestigated and are referred to here as electrokinetic geophysical sounding.

Potential applications of electro-acoustic measurements were noted, although the physics of the coupling mechanism between elastic and electromagnetic waves was poorly understood. Ivanov (1939) indeed surmised that electrical phenomena occurring in the Earth's crust during earthquakes are associated with such effects. This was later taken up by Mizutani et al (1976) and Ishido and Mizutani (1981) who provide an experimental and theoretical basis of electrokinetic phenomena in rock-water systems and discuss possible earthquake related effects.

Observational field studies of electrokinetic phenomena appear as 'intermittent' research papers in western journals in the 1950's (Martner and Sparks, 1959), the 1960's (Broding et al., 1963), the 1970's (Long and Rivers, 1975) and in the 1980's (Murthy, 1985). Soviet experiments are

described by Parkomenko (1971). The experiments include both laboratory and borehole investigations of electrokinetic effects (Parkhomenko and Gaskarov (1971). In 1993 two oil company researchers published the results of a systematic study of the potential of 'electroseismic effects' in the context of deep exploration for oil and gas (Thompson and Gist, 1993). The study, both theoretical and field based, predicted measurable electric field effects. The study concluded by suggesting the greatest potential for successful application lay in shallow exploration (e.g. for aquifers). In our studies which consider the potential of EK sounding for aquifer (and other) shallow investigations, the guidelines developed by Thompson and Gist (1993) have been followed.

4) THEORY

4.1) Porous rocks and streaming potential.

Natural porous materials are formed by various minerals such as silicates, oxides and carbonates. Such minerals develop an electrical double layer (EDL) when in contact with an electrolyte (Bockris and Reddy, 1970). The concept of the electrical double layer is illustrated in Figure 4.1. The EDL is made up of a layer of ions adsorbed on the surface of the matrix and of a diffuse mobile layer extending into the liquid phase. An electrical (zeta) potential exists on the first non-bound plane along which interstitial pore fluid is capable of movement (Overbeek, 1952). The zeta potential is illustrated in Figure 4.2. Typically the zeta potential may range from zero to values in excess of 150 mV (Pride and Morgan, 1991) and constitutes stored energy in the porous rock-mass. Electrokinetic coupling occurs under non-equilibrium conditions (e.g. when a pressure gradient is applied) and relative movement of the pore fluids results in a net displacement of charge across the EDL.

The relationship between differential pressure (∇P) and resulting electrokinetic voltage (∇V) is given by the Helmholtz-Schmoluchowski equation (Overbeek, 1952; Ishido and Mizutani, 1981)

$$\nabla V = C.\nabla P \qquad \text{.....(1)}$$

where C is referred to as the streaming potential coefficient. The streaming potential coefficient has been studied in the context of other geophysical methods of exploration such as self-potential and streaming-potential (Corwin and Hoover, 1979); typical values (-12 to over 350 mV/atm) in a variety of rock types are given in Ahmed (1964).

In the classical Helmholtz-Schmoluchowski equation, C is independent of any microstructural (pore) parameter and is given by :

$$C = \varepsilon\zeta/\eta\sigma \qquad \text{.....(2)}$$

where ε, ζ, η and σ are the fluid dielectric constant, the zeta potental, the fluid dynamic viscosity and the fluid electrical conductivity, respectively. The relationship assumes (i) the pore hydraulic radius (m) is >> than the EDL thickness, (ii) flow is laminar (for large m we expect non-linear/turbulent flow and (iii) surface conductance is small (<< pore fluid volume conductance).

In situations in which electrical surface conduction becomes significant (e.g. decreasing pore size, low conductivity i.e. fresh fluids) the streaming potential is modified as :

$$C = \varepsilon\zeta/\eta(\sigma + \sigma_{sc}) \qquad \text{.....(3)}$$

The additional term for surface conductivity (σ_{sc}) allows various microstructural parameters of the pore space such as porosity and permeability to be introduced (e.g. Ishido and Mizutani, 1981). Jouniaux and Pozzi (1995) describe laboratory experiments on sandstone and limestone samples in which the streaming potential depends on sample permeability; the dependence is strong when fluid resistivity is high and vice versa. Laboratory experiments (Revil et al., 1996) indicate that the magnitude of the zeta potential, and hence streaming potential, increases with decreasing electrolyte concentration so that the largest streaming potentials are associated with fresh (non-saline) fluid environments.

The subsurface property dependencies involved in electrokinetic coupling are not simple. The relationships suggest that all subsurface interfaces involving changes in the type of pore fluid (e.g. air or water), changes in rock type (giving rise to different zeta potentials), as well as microstructural properties (porosity and permeability) have to be considered.

4.2) The acoustic source

The theory for the propagation of the acoustic source follows the standard relationships of elastic wave propagation in an homogenous medium. An impulsive source, such as a hammer blow on a metal plate, propagating as a hemispherical wavefront with velocity $v = f\lambda$ (where f is frequency and λ is wavelength) is assumed. Initially the source is wide-band and f is multi-valued; frequency-dependent absorption will eventually produce a wavelet of dominant f and λ. One of the first elements of the wavefield to be examined is that connected with *vertical* propagation using ray theory.

The surface position of the source is referred to as the shot point. At a subsurface boundary, circular disturbances centred on the shot point are produced by the downgoing wave. As in the case of optics, the disturbances within even and odd numbered circular regions (Fresnel zones) with successive radii spaced one-half the wavelength apart are of opposite sign. The circular Fresnel zone, centred below the shot point is defined with approximate radius $r = (z\lambda/2)^{½}$ where z is depth. Figure 4.3 shows the variation with depth of the radius of the first Fresnel zone for uniform materials with acoustic velocities in the range 600 to 2400 m/s. At the frequency of 80 Hz shown (typical for a hammer/plate source), the radius may vary between 7 and 12.5 m at a depth of 10 m depending on the velocity of the near-surface layer.

The concept of a downward propagating sequence of first Fresnel zones, each capable of providing a radially coherent zone of displacement, is an important element of EK geophysical sounding. The idealised acoustic wavelet, since it is a minimum-delay function, is that due to Ricker (1953). The Ricker wavelet is the standard function for a pressure source. The expression for the wavelet is analytic and the time-domain behaviour is shown in Figure 4.4 for the three frequencies of 500, 200 and 100 Hz. For typical hammer/plate source frequencies (100 Hz and below) it is evident that wavelet durations extend to 20 ms and greater.

Ray theory provides a standard reference for the various types of compressional seismic waves typically generated by a pressure source (Dobrin and Savit, 1988). Figure 4.5 is a schematic time-distance diagram with the various seismic waves plotted with respect to the time at which they would appear on a field seismograph. Ground-roll effects, produced by dispersive Rayleigh

waves, can be significant in shallow studies. Ground-roll is distinguished on seismic records by a high amplitude and low frequency waveform. The waves travel along the ground surface (their amplitudes decrease exponentially with depth) at a velocity of about 0.36 that of compressional waves (Dobrin and Savit, 1988).

It is important first to note that in the case of a compressional acoustic wave propagating through a *homogenous* porous material, electrokinetic coupling produces a constant electric field confined to the wave (Fitterman, 1978; Pride and Haartsen, 1996). Independently propagating electromagnetic waves are not generated. When the acoustic wave traverses a boundary separating regions with different streaming potential coefficient then a charge separation that oscillates at the acoustic frequency is produced. This charge oscillation generates an electromagnetic field that can be observed at the surface. From the previous equations, the magnitude of the field will depend on the electrochemical properties of the rock/fluid and the mobility of the pore fluid.

In order to further understand the behaviour of electrokinetic phenomena, the fully coupled behaviour of elastic and electromagnetic wave interactions in porous media must be examined. The theories of quasi-static and dynamic poroelasticity for fully saturated media were presented by Biot (1956, 1962) and are the classical papers on the subject. More recent descriptions of Biot theory in relation to electrokinetic effects are given by Neev and Yeatts (1989), Pride (1994) and Pride and Haartsen (1996). From Biot theory, pore fluid participates in the rock motion (induced by an acoustic wave) due to viscous friction and inertial coupling. In the steady-state (plane-wave) case, Biot theory suggests two different mechanisms for converting the acoustic wave oscillation into relative fluid-rock motion thereby allowing the generation of an electrokinetic charge separation. In both cases, the fluid motion can be described as a Darcy particle velocity by analogy with Darcy's law for fluid flow in a porous medium.

The first conventional Biot wave (the so-called fast wave) produces rock and fluid motion which are in-phase and the Darcy velocity is determined primarily by fluid viscosity and permeability. Biot theory also indicates that an acoustic wave is partially converted into a 'slow' wave at an interface. The slow wave is highly dispersive and attenuates rapidly on a typical scale of much less than 1 m (Thomson and Gist, 1993). Despite the rapid attenuation, the slow wave is capable of generating a large Darcy velocity typically greater than that generated by the fast wave through a high permeability formation (Thomson and Gist, 1993). In principle, the dispersive nature of the slow wave implies a capability for high vertical resolution.

Although both waves may produce relative rock-fluid displacement capable of generating electrokinetic coupling the effective area and volume contributions will differ in the two cases. In the case of a downgoing hemispherical wavefront incident on a tabular horizon the anticipated electromagnetic response due to electrokinetic coupling is a vertical electric dipole oscillating at the same frequency as the acoustic source. The area across which the acoustic oscillations are coherent is the first Fresnel zone. The magnitude of the dipolar field is usually expressed by its moment i.e. the product of current and volume. In the case of fast wave coupling, the volume may be expressed as the product of the area of the first Fresnel zone and the formation thickness. In the case of slow wave coupling the volume would be expressed as the product of the area of the first Fresnel zone and the slow wave attenuation length.

4.3) The vertical electric dipole

According to the above description, the geophysical signature of electrokinetic coupling due to vertical acoustic wave propagation will be that of a vertical electric dipole (VED) centred directly below the shot point. An important feature of the coupling is that the electromagnetic oscillation will propagate to the surface at the speed of light. At a given depth, the time instant of coupling will occur at the one-way transit time of the downgoing acoustic wave.

The behaviour of the fields associated with a buried VED can be investigated by numerical modelling. To alleviate the problem of prescribing a field situation, the calculations are done using a point source VED with unit dipole moment. A cross-section through the earth showing contours of the horizontal electric field (Ey) due to a VED at a depth of 10 m is shown in Figure 4.6. The relevant parameters of the model are a frequency of 80 Hz, a uniform half-space of resistivity 100 ohm.m with a relative dielectric constant of unity. In Figure 4.6, a banded colour scheme is used to emphasise the field gradients.

The Ey field exhibits dipolar field symmetry about the acoustic source location (y=0) which represents a field null point. Maximum at-surface field magnitudes occur, symmetrically, at y=-5 and +5 m i.e. at half the depth of the VED source. For a subsurface dipolar source, maximum surface amplitudes will always be observed at an offset equal to half the depth of the source. Equally important is the phase reversal (180 degrees) of the field oscillations occurring about the plane of symmetry (y=0). The phase reversal is highly significant in that all other sources of electromagnetic radiation (natural and anthropogenic), which may interfere with the measurement, are 'distant' and would appear as in-phase oscillations across the 'local' scale of the measurement depicted.

Although equivalent bipolar magnetic field behaviour is generated by the VED source, the magnitude of the at-surface magnetic field (Hx) oscillations is expected to be very small. In the example shown, the maximum Hx field is 750 picoTesla. Such fields are too small to be routinely measured with current geophysical field magnetometers. It therefore appears that surface measurements of the horizontal electric field (for which geophysical devices with adequate signal/noise exist) are appropriate for investigations of electrokinetic coupling.

The horizontal electric field cannot be measured at a point. The gradient of the potential (P) across two grounded electrodes is the routine method of measurement since $E=-\nabla P$. In practice a very small electrode separation (e.g. < 1m) may result in low signal/noise while a large separation may average the field gradients defining the spatial form of the field. Some form of compromise is inevitable. The problem is studied by extending the analysis of the VED to various depths and examining the signals obtained at various positions along the surface. The locations are best described as a horizontal offset from the source (acoustic shot) position. A common feature of the VED analysis is that the maximum field strength is observed at an offset equal to one-half the depth of the VED source. For the analysis ‘virtual electrode separations’ of vanishingly small length are assumed.

Figure 4.7 shows the variation of the horizontal electric field at 4 offset positions (2, 4, 10 and 20 m) for VED depths of between 1 and 50 m. The moment of the VED remains constant (1 A.m) at all depths. At first sight the response behaviour of individual offset locations shown in Figure 4.7 may appear counter-intuitive. Although, as discussed previously, the maximum surface field amplitude is generated at an offset equal to one-half the source depth, for each specific location a maximum response is observed when the source depth is one-half the offset distance.

From Figure 4.7 it is evident that small offset locations provide (i) the largest field amplitudes, particularly for near-surface VED sources and (ii) the highest degree of depth sensitivity. For the example used (constant dipole moment with depth), field amplitudes from deeper sources of coupling (e.g. > 20 m) will provide similar amplitudes at both near (2 m) and far (20 m) offsets. For a VED source at 50 m depth, the field amplitude at 2 m offset is reduced by less than one order of magnitude from that at an offset of 20 m.

Thus while it is possible to envisage multi- channel systems capable of measuring Ey at sequential offsets, the most effective and sensitive measurement location occurs in the immediate vicinity of the shot point. In order to accurately measure the field gradients from possible shallow sources it is clear that very small electric dipole lengths (e.g. 1 or 2 m) are required.

Although it might be construed that an extensive array of offset measurements would be required to locate a position of maximum field strength and thereby a depth to source, this is not strictly necessary if an alternative characteristic of electrokinetic coupling is exploited. As described previously, the time-instant of coupling will occur at the one-way transit time of the downgoing acoustic wave. Thus if the acoustic velocity structure is known, or can be estimated, then the time-instant of coupling can be converted to an equivalent depth (assuming coupling at interfaces due to vertical P-wave propagation).

4.4) Predictions from theory

The previous section provides a simplified assessment of the spatial form and relative amplitude of surface voltages due to a VED. In order to describe the behaviour of electrokinetic phenomena, the fully coupled behaviour of elastic and electromagnetic wave interactions in porous media must be examined. The theory and practical application through numerical methods are beyond the scope of the project. It is however possible to make simplifying assumptions, especially about the acoustic source, in order to arrive at some estimates of signal amplitudes.

Two simplified methods for the prediction of surface electric potential due to a subsurface interface providing a change in streaming potential coefficient have been examined. Both methods are effectively steady-state at a single source frequency. Both methods assume simple vertical propagation of the acoustic wave with coupling taking place within a Fresnel zone ‘volume’ as described previously. The algorithms are mathematically intense and both require a large number of parameters to be specified for a given hydrogeological situation. The details of the work will be reported elsewhere.

The first method uses the basic equation (2) and the capillary model of Ishido and Mizutani (1981) and requires the specification of porosity and tortuosity in addition to the rock parameters of equation (2). The second method follows the work of Fitterman (1978) and predicts the surface potential due to a spherical pressure gradient coupling with a boundary separating two regions of different streaming potential coefficient. A large number of petrophysical parameters must be included to arrive at a prediction for even a simple two layer model. Sample calculations

for different groundwater models using typical hammer energy sources and for interface depths from the near-surface to 50 m have been undertaken. The results indicate that it is possible to predict a wide-range of surface amplitudes, from several microvolts to values in excess of 1 mV/m, in the near-vicinity (< 5 m) of the shot point, depending on the petrophysical parameters chosen for the hydrogeological model. While such predictions confirm that EK signal levels in the micro-to-millivolt range can be expected, the modelling results are highly non-discriminatory.

To emphasise the difficulties of quantitative prediction of signal amplitudes, the joint-waveform modelling and field-data comparisons presented by Mikhailov et al (1997) can be referenced. The work relates to the shallow near-surface and considers a 3-layer above bedrock situation. The 3-layers consist of (i) top-soil (thickness 0.76 m), (ii) unsaturated glacial till (thickness 2.44 m) and (iii) saturated glacial till (thickness 6 m). The electrical and mechanical parameters that must be specified (for each layer) are more extensive than those of our own modelling and comprise:

porosity, permeability, bulk modulus of the solid, bulk modulus of the fluid, bulk modulus of the frame, shear modulus of the frame, viscosity of the fluid, density of the solid, density of the fluid, salinity of the fluid, temperature, permittivity of the solid, permittivity of the fluid and tortuosity.

It will be appreciated that the majority of these parameters are site (hydrogeological model) specific and include 'difficult' microstructural rock specifications such as permeability and tortuosity. In addition, a number of the parameters (e.g. density and permittivity) depend on the degree of water saturation and this must also be specified for each layer.

The modelling (both acoustic and electrical) relates to the single near-surface boundary between the top soil (2% water saturation assumed) and the unsaturated glacial till (20% water saturation assumed) at a depth of only 0.76 m. The results obtained by the authors are **highly significant** in relation to our own assessments of EK behaviour. The results of the modelling are reproduced here in Figure 4.8, after Mikhailov et al (1997). The main limitation of the modelling is that there is no free surface (just a single interface).

To allow sufficient separation of the different effects, a Ricker wavelet with a 300-Hz centre frequency was adopted. This has the effect of confining the acoustic pulse widths to less than 10 ms in the results of Figure 4.8. If a more realistic, lower frequency was adopted (i.e. more typical of a hammer/plate) then the effect would be to increase individual pulse widths by a frequency scale-factor. For an acoustic frequency of 100 Hz, the pulse width would increase by a factor of three (e.g. to 30 ms). The simple P-wave EK conversion at 0.76 m is the first negative pulse observed simultaneously across the dipoles (labelled A-A); the amplitude has a rapid decay with offset. Within 3 m of the shot-point (10 ft) it can be seen that the EK record is dominated by later events all possessing moveout. Event B-B is identified as the head-wave travelling along the shallow interface. The two later events are identified as a refracted shear (S) wave and a reflected P-wave. In summary, the important elements of this limited modelling indicate:

The near-shot record is dominated by a variety of voltages due to 'additional' acoustic wave interactions (e.g. head and reflected waves). The additional voltages possess spatial moveout and converge and are superimposed near the shot location.

If the same results were extended to a lower frequency, more representative of a hammer/plate combination, a complex EK voltage record extending towards 40-60 ms could be generated from a single interface at a depth of a few metres.

By definition, the only way to identify a 'simultaneous' EK signal due to vertical P-wave propagation is to obtain measurements at increasing offsets. The identification of 'simultaneous' behaviour is likely to be obscured by the superimposed effects of additional acoustic wave interactions.

By extension of the single-interface results, a multi-layered environment will inevitably give rise to a much higher level of complexity both in the acoustic wave interactions and the resulting superimposed EK coupling effects.

5) TWO-CHANNEL EK SOUNDING

The 'two channel' approach to EK sounding forms the basis of the instrument and methodology initially used for the field evaluations. The instrument and associated interpretation procedures are well explained in the user manual that accompanies the equipment. The basic investigation of the EK effect concerns the time-dependent behaviour of the voltages that are recorded by symmetrical surface dipoles. The concept introduced by the suppliers is that the voltage returns observed on the two dipoles can be interpreted **entirely** by Fresnel zone coupling vertically beneath the shot point.

According to the user-manual a conceptual model for EK behaviour consists of a 3-layer subsurface. Layer 1 is an at-surface layer which defines the depth to a fully-saturated formation (e.g. an aquifer). If this first layer is impermeable or contains no pore fluids, no EK signal can be generated. Layer 2 comprises a zone from which an EK response may be observed given one or more fluid-filled permeable horizons. Layer 3 underlies layer 2 and allows a bedrock/basement to be defined. This conceptual model forms the basis of the interpretation software. The layers must be assigned known or estimated seismic velocities and thicknesses in order to convert the recording time of an EK measurement into depth. The recording and interpretation concepts are illustrated in Figure 5.1.

Clearly the above conceptual model is simplistic. Our initial assessments were based on the EKS Operating Manuals (V.2, March 1995 and V.3, September 1995) and an initial 'hands-on' 3-day training course with the manufacturers. The salient operating/processing/interpretation points (from the manual) are now discussed.
The manual states: 'The EKS equipment is designed to carry out the following tasks with the operator adjusting a few parameters: data acquisition, converting signal acquisition time to depth, estimation of depth to water table in unconfined aquifers, average aquifer porosity, depth and thickness of confined aquifers, aquifer permeability versus depth, depth to basement, depth to

water-filled ‘fracture zones’ in basement and predicted borehole water flow for a given well depth and threshold permeability.’

In terms of assessment it seemed reasonable to subdivide the procedures into the three stages shown in Figure 5.1. The 3 stages shown can be considered geophysical and aim to provide porosity and permeability as a function of depth. Given such information further predictions, such as borehole yield, become hydrogeological. In large part, our main assessment priority has been to consider the stage 1 to stage 2 transformation i.e. converting the data from time to depth. If this transformation is in error, all the subsequent information becomes unsafe.

The rules for identification of EK signal and noise components are defined in the manual and examples given. Further examples can be found in the manufacturer’s promotional literature. **Where the example recordings are shown against time, the signals occur in the first tens of milliseconds**. In terms of data interpretation of the water table, the manual suggests: ‘*A comparison of the two signals displayed on the GROUNDFLOW LOG will reveal the water table depth if the aquifer is unconfined. This is because the symmetry of the electrokinetic signal pattern is such that the two signals will be in phase; a peak on one channel will correspond more or less exactly to a peak on the other. Electrokinetic signals from below the water table always have this characteristic. Noise voltages from above the water table have the same polarity characteristics as distant noise. That is, the signal on one channel will be more or less out of phase with the signal on the other; the signals will be moving in opposite directions. Furthermore, the patterns above the water table will differ markedly from shot to shot.’*
Where the aquifer is confined the manual suggests ‘*... there may be no indication of a water table and all the electrokinetic signal is in phase. The top of the aquifer is indicated by a transition from nearly zero signal to the first event, in such circumstances.’*

Especially for overseas use, assessments of the ‘simple’ identification of the water table were given priority. The identification of the ‘water table’ is **CRITICAL** to the stated methodology. The water table ‘position’ (its time in milliseconds) must be identified from the ‘raw’ voltage data. This position (in time) forms the first, non-aquifer layer. The time position is converted to depth using a user-assigned velocity of the uppermost layer.

According to the above description, an EK 'signal' may be identified as time-dependent behaviour which is 'in-phase' on the two electric dipoles placed symmetrically about the shot point (the actual polarity of one of the dipoles having been reversed). An EK signal must also be repeatable over successive recordings (hammer shots). The degree to which the time behaviour of the two channels can be identified as 'in-phase' is part of an EK interpretation. The methodology proposed in the manual was to take several shots and to ‘select’ one for interpretation. No data stacking is possible and the suggested procedure requires the mental comparison of several recordings. The assessment procedure adopted in this project was that the repeatability of any received signal must be demonstrated. This would allow the identification (and rejection) of poor/inadequate data and the construction of a ‘stack average’ from a series of repeated soundings.

During the first 12 months of the project, 6 revised versions of the software were issued by the suppliers to overcome a series of errors and bugs. Since all but the first task (data acquisition) required evaluation (subsequent procedures were not explained in any detail) the supplied equipment and software was used only for the first task i.e. data acquisition. A suite of in-house software routines and graphical displays was written to perform data processing and interpretation and to exercise full control of the sounding data. A translation program allowed the conversion of the processed data back to the manufacturers 'raw data' format.

5.1 Estimation of porosity/permeability.

The concepts and methods used to estimate porosity and permeability from an interpreted voltage/depth sounding curve are described by Millar and Clarke (1995) under the heading *dynamic electrokinetic effects*. The authors argue that the acoustic 'pulse' of given shape is distorted during propagation to depth, but then electrokinetic coupling then alters the shape further. The results of a single laboratory study (Chandler, 1981) are then used to relate electrokinetic rise-time to porosity and permeability. To apply the results of Chandler (1981) it is necessary to specify a number of rock parameters including : *porosity, bulk modulus of the solid, bulk modulus of the fluid, bulk modulus of the frame, shear modulus of the frame and viscosity of the fluid.* It will be recognised that these parameters form a subset of the previous modelling parameters. They are clearly site-specific.

Millar and Clarke (1995) say: 'The EKS signals obtained by our equipment yield returning pulses from formation layers which may be distorted because of these risetime effects. If formation interfaces are sharp on a length-scale (< 1 m) corresponding to less than a risetime, then such EKS data could be processed to deduce risetime and infer permeability, if porosity and elastic moduli were estimated'. The authors go on to note that the approach adopted is 'ambitious'.

The clear problem with the ambitious approach adopted is that the voltage response is a convolution of the seismic pulse with the interface causing coupling (assuming vertical propagation). The conventional view of the seismic pulse is that it conforms to a Ricker wavelet as shown previously in Figure 4.4. A modified/distorted form of the theoretical wavelet is indeed 'reflected' in many of our voltage data sets and in other recent publications (Butler et al., 1997).

The rise-time of an EK response will primarily be determined by that of the seismic wavelet. Secondary level modifications to the wavelet will arise due to propagation and interaction with interfaces. It is suggested that any subsequent modifications to the time-history of coupling due to electrokinetic rise-time effects (as per the Chandler laboratory results) would amount to only third-order effects. In order to effectively apply the Chandler theory to the voltage recordings it would be necessary to eliminate (deconvolve) the primary and secondary (propagation) effects in the source wavelet.

In our opinion the rise-time of the EK voltage recordings are, primarily, a reflection of the behaviour of the acoustic source rather than being a measure of the permeability of the subsurface. Following on from this, the estimation of hydrogeological parameters of an aquifer (part of the methodology) which is based on the use of voltage rise-time appears to be a highly questionable exercise.

In general the estimation of permeability and other aquifer properties has not been a priority in the current project although our data presentations have included the rise-time behaviour of the recordings. One example of a detailed attempt to estimate permeability at a hydrogeological test site is provided later. The example is used to illustrate the difficulties and 'circularity' of such procedures.

5.2 Field experiments overseas.

The main overseas assessments of the technique under project R6232 took place in Zimbabwe (November 1995) and in Egypt (April 1996). An earlier 'opportunistic' use of the technique took place in Vietnam (June 1995, under the Unconsolidated Sedimentary Aquifers Project) soon after the equipment was purchased. The earliest work was reported in Peart et al. (1995).

The work in Zimbabwe is reported by Beamish et al. (1997). This report gives many examples of the technical/experimental tests that were carried out. The report describes the geophysical and hydrogeological data that were obtained in the three main environments studied. Typically in the survey classification scheme used, the following comments apply to the data obtained :

(i) Borehole sites : generally low amplitude, spatially inconsistent and difficult to interpret.

(ii) Collector wells : a variety of types and magnitudes were observed, ranging from small to large amplitudes.

(iii) Sand rivers (drainage courses incised in former pluvial periods and subsequently infilled) : moderate to large amplitudes. The soundings display high levels of spatial consistency.

The major effort was expended in assessing and improving the quality and reliability of the data. The three main conclusions concerning data quality were :

- Data stacking (of repeated shots) to identify/reject poor data and to confirm the validity of a response should be used routinely.

- The presence of high electrode contact resistances (indicated as acceptable in the manual) degrades EK data. To improve data quality in arid environments, metal electrodes should be watered or porous pot electrodes should be used.

- Single 'spot' EK soundings should be avoided. In general there appears to be sufficient 'near-surface' complexity to warrant detailed traverses and/or azimuthal assessments of sounding behaviour.

The latter point is important. If, as the manual suggests, the interpretation of the data proceeds according to a model of tabular (1D) 'horizons', then it is possible to investigate the degree to

which this model is appropriate by undertaking additional measurements, using the same shot point but at different azimuths. The most obvious arrangement is to repeat a sounding at a 90 degree azimuth. In cases where information from deeper horizons (e.g. ten metres and greater) is sought it is also possible to undertake additional soundings along a profile to confirm the validity of both data and interpretation. For a 2-channel electrode spread length of 5 m, profile observations become 'contiguous' for a sounding separation of 5 m. Many other experimental configurations are clearly possible.

Figure 5.2 (from Beamish et al., 1997) shows the type of differences that can be observed by azimuthal soundings in the vicinity of a borehole. In our opinion these data are inconsistent and interpretation cannot proceed. In other situations (e.g. Peart et al., 1997a) azimuthal soundings have provided consistent data.

The most spatially consistent data were obtained by performing traverses across sand rivers (Beamish et al., 1997). The profile observations were generally performed at sounding intervals of 20 to 30 m. The sounding characteristics were similar across each traverse and across different traverses (separated by 70 km). Figure 5.3 provides an example of the data obtained with the main voltage oscillations taking place largely within the first 20 ms of the sounding. The water tables in the vicinity of the sand river profiles were shallow, typically 3 to 10 m. To first order the data obtained appear to be consistent with the limited knowledge of the hydrogeology.

The Zimbabwe soundings made near boreholes generally produced poor quality data so that detailed comparisons with hydrogeological control were not justified. The more limited survey in Egypt (Peart et al., 1997b) did however provide clear evidence of the failure of carefully-controlled soundings to 'detect' hydrogeology. Large amplitude signals were observed and clearly generated in zones of partial saturation while an underlying high permeability aquifer at a depth of only 22 m yielded no visible response. At other sites, relatively strong signals were recorded above clay-rich units and a complete absence of signal was observed above both shallow and thick saturated aquifers.

5.3 Field experiments in the UK

A large number of experimental soundings have been conducted in the UK. During the later half of the project, increasing use was made of multi-channel data acquisition and seismic data were also acquired in conjunction with the EK observations. These data were part of a series of critical experiments that were performed to enhance our basic understanding of EK coupling. Prior to these experiments, assessments were carried out using simple extensions (e.g. profiling) to the 2-channel methodology. Some of these data are now discussed.

Figure 5.4 shows a typical two channel EK recording above the Sherwood Sandstone aquifer capped by 0.5 m of Boulder Clay. The water table is at a depth of about 25 m. The sounding was repeated on two different dates. The only significant processing applied to these data is the removal of 50 Hz mains and its harmonic components. In each case, three individual shot records are shown from two shot-symmetric 2 m dipoles. The broad form of the soundings is similar on both dates and on each date the individual shot data are highly repeatable. The data on the earlier recordings contain some higher frequency components that are not immediately apparent on the second date. In both cases the data across the initial 2 to 3 ms of the recording display out-of-phase behaviour.

Spectral analysis of the data in Figure 5.4 confirm the main energy component of about 80 Hz. The form of the large amplitude oscillation is thus consistent with a 'modified' theoretical Ricker wavelet at this frequency (e.g. Figure 4.4). The onset time of in-phase behaviour occurs at 2 to 3 ms and thus **cannot** be associated with the water table (for any reasonable acoustic velocities of the clay/sandstone). The conclusion reached is that a shallow interface is responsible for the coupling. If a response from the water table is sought at later times, it is clearly difficult to extract (in our opinion).

The next example comes from a hydrogeological test site (Hall Farm) which provides a high degree of subsurface control including hydraulic conductivities estimated by both in-situ (pump) testing and by laboratory determination. The geological sequence at Hall Farm comprises cover sand resting on Lowestoft Till (Anglian age) which in turn overlies the Cretaceous Upper Chalk. The borehole lithology log indicates a sequence of :

Sand (0-2.25 m), Oxidised Clay (2.25 to 7.60 m), Un-oxidised Clay (7.60 to 14.35 m), Oxidised Clay (14.35 to 20.29 m) on Chalk (at 20.29 m).

Although a profile of contiguous observations was obtained, the results discussed here are taken from the sounding in the vicinity of the borehole. Some of the sounding data (several repeat shots) are shown in Figure 5.5 and a large (negative) amplitude signal is clearly associated with the at-surface sand unit. This behaviour has been recorded in other UK environments possessing a partially/fully saturated cover sand. In order to accurately convert sounding time to depth, knowledge of the subsurface acoustic velocities is required. To some extent, knowledge of subsurface formations is also required since they will influence the distribution of acoustic velocities encountered. The geological sequence above was used as control to assign a velocity structure that enables EK-estimated hydraulic conductivities to 'match' the main features of the 'control' information.

The field conductivities are shown in Figure 5.6. The two features of Figure 5.6 which were used to estimate seismic velocities were (i) the low hydraulic conductivity associated with the base of the sand unit and (ii) the profile minimum associated with the un-oxidised Clay unit. The seismic velocity model comprised three layers : (1) Layer 1, Sand, 0 to 2.25 m, (2) Layer 2, Clay, 2.25 to 20.29 m and (3) Layer 3, Chalk. In practice only the velocities of Layers 1 and 2 were adjusted (within appropriate ranges) to obtain an approximate match to the two control depths. The final seismic velocities used were Layer 1 (Sand) : 800 m/s, Layer 2 (Clay) : 1600 m/s and Layer 3 (Chalk) : 2200 m/s. Clearly the assignment of a 'single' velocity to all three Clay units (which show rapid variation in hydraulic conductivity) is simplistic.

The comparison of the pump-test hydraulic conductivity results and those estimated from the EK sounding is also shown in Figure 5.6. When comparing the results in detail, the limited dynamic range of the estimated hydraulic conductivities should be noted. The experimental estimates were limited, by the dynamic range of the data acquisition system, to less than 3 orders of magnitude and are restricted to the range from 0.01-0.1 to about 10 m/d. EK-estimated hydraulic conductivities of less than 0.1 m/d (say) imply low permeabilities but 'true' values are not accurately determined.

It is possible to argue for 'good' and 'bad' correspondence within the comparison of hydraulic conductivities obtained. It is stressed that the control information was used to obtain a 'best-fit' of the EK sounding data. The point at issue is the extreme difficulty in converting time-to-depth even when a high degree of subsurface control exists. Since individual acoustic velocities may be

assigned values that are bounded by factors of 2 or greater, when multiple velocities are assigned, errors in depth estimates accumulate.

A third example is taken from sounding characteristics on clays. Clay environments have consistently returned some of the smallest amplitude voltages that have been observed during our assessments in the U.K. This simple observation is in accord with electrokinetic theory in that, if it assumed that clay environments represent a low permeability medium, then lower amplitude EK coupling is anticipated. In practice, the subject of water in clays and electrokinetic effects is highly specialised. In contrast to non-argillaceous rocks, clays contain additional intermolecular bonding forces that are likely to further impede EK coupling.

A 100 m profile of contiguous 5 m soundings was obtained over an area of Boulder Clay which was apparently uniform over a few square kilometres. A Coal Board borehole indicated 40 m of Boulder Clays overlying Lias clays/mudstones. Figure 5.7 shows four 2-channel soundings obtained at 15, 20, 30 and 35 m along the profile. The magnitudes of the voltages are typically < 1 mV/m. Despite the small magnitudes, the data display in-phase 'signal' characteristics over the first 20 ms of the records. In the more complex record obtained at 35 m, it can be seen that one of the channels retains the sounding characteristics of the previous records.

The two channels of data along the entire profile are shown as colour-contoured time sections in Figure 5.8. Relatively large (> 0.2 mV/m) amplitudes at individual locations dominate the section. In part, some of these larger amplitude excursions occur in only one channel and correspond to the 'inconsistent' one-channel behaviour of the previous figure. In other portions of the profile, particularly between profile distances of 15 and 40 m, spatially-consistent, in-phase coupling is observed over the first 20 ms of the data.

This, and other, studies on clays were intended to provide a 'limiting case' of a low permeability environment. A 'null' (no EK coupling) response has NOT been observed, although the general 'clay' response is clearly of low amplitude. The fact that coupling occurs indicates an interface in streaming potential coefficient. It is then necessary to speculate that the clay is non-uniform and may contain sand/gravel deposits that constitute such an interface.

.

The pervasiveness of EK coupling effects such as those discussed above, from a wide variety of hydrogeological environments, together with the lack of a simple signature from the water table, has led to far more extensive field experiments to spatially map the behaviour of *both* the acoustic and electromagnetic fields in the vicinity of the shot point. These critical experiments are now discussed.

6) MULTI-CHANNEL EK SOUNDING

The voltage returns that are observed are clearly associated, in some manner, with the passage of the seismic wave away from the shot point. Clearly the use of only two channels is not discriminatory in terms of describing the complete spatial/temporal nature of the voltages generated. It has been necessary to extend the observations to multi-channel measurements at various offsets from the shot point. This type of 'move out' experiment is common in seismic refraction studies which use an offset spread of geophone receivers to investigate the subsurface acoustic velocity structure.

A further in-house BGS activity has been the development of an 8-channel EK instrument named TEKA (Transient EK Array). The system has an increased dynamic range of 16-bits and gains from 200 to 1600. The TEKA system allows both dipole and geophone sensor input and was designed to investigate the smaller microvolt EK coupling effects predicted by theory. Increasing use was made of the system during the later stages of this project.

In the case of EK moveout experiments, the seismic geophones are replaced by pairs of E-field dipoles. In practice such move out experiments are duplicated using both geophones and dipoles to allow examination of both acoustic and voltage behaviour. During the course of our assessments descriptions of other multi-channel EK experiments began to emerge in the literature (e.g. Dietrich et al., 1996; Butler et al., 1997).

In practice any conventional seismic source when interacting with the subsurface generates both body and surface waves. The body waves may include compressional and shear components and both refracted and reflected waves can be generated by interfaces (acoustic contrasts) and observed at the surface. Surface or Rayleigh waves (e.g. ground roll) are generated along the free surface and are typically low frequency, low velocity waves. This site-dependent complexity of acoustic behaviour has two main geometrical implications for EK experiments. The main implications concern EK coupling due to vertically propagating waves (as discussed previously) and those due to horizontally propagating waves. The main horizontally propagating waves are the two surface waves (Rayleigh and direct) and the critically refracted head wave which moves along a subsurface interface and generates a charge separation across the boundary (Mikhailov et al., 1997). The EK oscillations associated with both surface and head waves would be detected at increasing times as the waves moved out from the source beneath an array of surface dipoles. This contrasts with instantaneous arrivals to be expected from coupling due to vertical propagation.

A schematic diagram showing the simplest concepts in (a) acoustics and (b) electrokinetics is shown in Figure 6.1. The diagrams shown are for a single interface and ignore surface waves, shear-waves and the complex reflection and refraction paths from more realistic multi-layered models.

The basic question to be addressed is to what extent the shot-symmetric voltages are caused by (i) lateral (horizontal) move out of the acoustic wave and/or (ii) vertical propagation. Both cases are capable of generating shot-symmetric behaviour (assuming tabular structure). In the first (horizontal propagation) case of surface wave effects, EK coupling would typically generate low frequency voltage oscillations (due to Rayleigh waves) and would be associated with the very low seismic velocities in the uppermost material (typically unconsolidated). Again in the first (horizontal propagation) case of head wave effects, EK coupling would generate voltage oscillations at the compressional wave frequency and be associated with the higher velocity of

the material below the head wave interface. In the second (vertical propagation) case, the voltage returns would be associated with the vertical distribution of acoustic velocities and would enable a 'vertical sounding' capability. Only in this second case would EK signals (if generated) propagate back from a subsurface horizon and appear as instantaneous events across an array of surface dipoles.

6.1) Case study 1. Sherwood Sandstone.

The mapped geology at this site shows shallow subcropping Sherwood Sandstone, generally coarse grained with bands of pebbles and occasional clay. Following trials with EK in the site vicinity, a main profile was established to examine both acoustic and voltage moveout behaviour. Prior to these experiments, the EK voltage behaviour as a function of dipole length was investigated using two-channel operation. Figure 6.2 shows the true voltage amplitudes that were obtained for dipole lengths ranging from 1 to 10 m, using a fixed inner electrode position at 0.5 m from the shot point. The channel 1 data, to the left of the shot, are shown in the upper frame and the channel 2 data (to the right of the shot point) are shown in the lower frame. The main amplitude oscillations are in the several millivolt range and it can be seen that the main voltage oscillations are independent of the dipole length (when the same inner electrode is used).

A small-scale seismic refraction experiment was carried out using a spread length of 35 m. The shallow velocity structure was determined as 306 m/s to about 8 m depth, underlain by material with a velocity of 800 m/s. A detailed EK moveout experiment was conducted in the centre of the profile. Dipole lengths were reduced to 50 cm and soundings were obtained using 2 symmetric dipoles. Soundings were repeated using dipole centre offsets of 0.5 to 3.5 m from the shot point. The channel 2 data (i.e. to the right of the shot point) are shown as normalised wiggle traces in Figure 6.3. This form of display is common in the presentation of seismic data. It is clear from the display that there are no ‘simultaneous’ arrivals in the voltage data

The use of small dipole lengths (< 2m) is adequate when the voltage amplitudes are in the millivolt range, as at this site. Their use enables a high degree of lateral resolution of moveout effects. Standard two-channel operation typically uses 2 m dipoles with a centre at 1.5 m from the shot point (i.e. electrodes at 0.5 and 2.5 m). Such data would be represented here by the display at 1.5 m. Figure 6.3 reveals that at locations both less than and greater than this centre, moveout effects can be detected in the main voltage oscillations. Also, the lateral resolution is sufficient to detect the onset of an additional positive oscillation at 26 ms at an offset of 2 m. This oscillation also has a clearly defined moveout over the limited spatial scale of the measurements.

The behaviour of the two channel data is summarised in Figure 6.4 which shows the trace normalised voltage data as colour-contoured time sections. The two shot-symmetric data channels show a high degree of coherence (in-phase behaviour) about the shot point and moveout behaviour is associated with all the main oscillations. The apparent velocities are very low and range from 350 m/s to 120 m/s.

6.2) Case study 2. Sherwood Sandstone.

At this site the mapped geology is Boulder Clay which is thin (< 10 m over the survey area) and overlies Sherwood Sandstone. Following trials with EK in the site vicinity, a main profile was established to examine both acoustic and voltage moveout behaviour. Prior to these experiments,

the EK voltage behaviour as a function of electrode-type was investigated using two-channel operation. Figure 6.5 shows the true voltage amplitudes that were obtained using stainless-steel (standard) electrodes, lead rods and non-polarising Cu/CuSO4 electrodes. Dipole lengths were 2 m and were centred at 1.5 m from the shot point. Similar characteristics are observed in all three soundings with only partial 2-channel in-phase behaviour reproduced in all three cases. The EK voltages are in the millivolt range and signal is observed down towards 80 ms suggesting the location warranted further investigation.

A full-scale refraction experiment was carried out using a spread length of 100 m. The end shots (at -0.5 and 100.5 m) proved competent rock with velocities in the range 2890 to 3203 m/s at depths between 16 and 25 m. This is overlain by a layer of velocity 800 m/s which is in turn covered by unconsolidated material (velocity of 365 to 560 m/s) about 5 m thick.

A joint EK/acoustic moveout experiment was conducted in the centre of the profile. Dipole lengths were reduced to 50 cm and soundings were obtained using 2 symmetric dipoles. Soundings were repeated using dipole centre offsets from 0.5 to 6 m. The data from the EK moveout experiment are shown as normalised wiggle traces in Figure 6.6. An onset time of 4 ms is used to avoid normalising by the large early-time (0 to 4 ms) oscillation that occurs on all traces.

As in the previous case, Figure 6.6 reveals that at locations both less than and greater than a 'standard' centre of 1.5 m, moveout effects can be detected in all the main voltage oscillations. The behaviour of the EK moveout data is summarised in Figure 6.7 which shows the trace normalised voltage data as a colour-contoured time section. Although the data show a degree of coherence (in-phase behaviour) about the shot point some asymmetry is also evident with 'faster' apparent velocities observed at positive offsets. This form of display also reveals that the weaker voltage oscillations at later times (towards 100 ms) also display moveout at similar velocities to the earlier voltage oscillations. The apparent velocities are low and range from 350 m/s to a maximum of about 500 m/s.

The acoustic experiment duplicated the EK experiment with 10 Hz geophones placed at 0.5 m intervals. The acoustic data are shown as normalised wiggle traces in Figure 6.8. The first, high frequency arrival observed on the traces is the air-wave from the hammer/plate combination with a velocity of 330 m/s. Subsequent arrivals, including the direct wave, are of similar low velocity and do not exceed 400 m/s. Below the air-wave, the first arrival displays non-linear moveout as the shot-point is approached (i.e. at offsets < 3 m). Towards later times, a much slower arrival is detected (about 140 m/s). This arrival is likely to be a surface wave. In detail, the acoustic data display a degree of asymmetry (about the shot point) similar to that of the voltage data.

Routine spectral analysis (e.g. Fourier analysis) of both voltage and acoustic data has been carried out. Since the main energy components are low frequency (typically below 200 Hz) it has been necessary to carry out more sophisticated (higher resolution) techniques to resolve the lower frequency components present in the data. Figure 6.9 shows the power spectrum obtained from the voltage data at offsets of 1 to 5 m. The dominant energy occurs at frequencies of less than 100 Hz. There is some variation in peak frequency with offset however the main energy components occur across a narrow band between 40 and 70 Hz. The corresponding results for the acoustic data are shown in Figure 6.10. For these data, the peak energy components occur between 40 and 60 Hz and the power spectrum displays more structure towards higher frequencies.

6.3) Case study 3. Gore Sand River, Zimbabwe.

A number of joint moveout experiments carried out overseas are discussed in Peart et al. (1997a). These experiments were carried out in the Bikita District of southern Zimbabwe as part of an extension to project R6232. The results from the experiment at the Gore Sand River are now discussed. The Gore Sand River channelway is incised into crystalline basement rocks (largely granite). The river is about 15 m wide and infill is thought to be about 6 m thick.

Figure 6.11 is a summary of the 'typical' dual field moveout behaviour observed in the immediate vicinity of a shot point. The experiment is highly detailed (E-field dipole lengths of 1 m) with both sets of measurements obtained at intervals of 50 cm. 10 Hz geophones and a data acquisition rate of 20 kHz were used. The two sets of results have been treated identically using individual trace normalisation (to +1 and -1) across the 100 ms time window shown.

The seismic data, colour-contoured in the left frame, display time-offset gradients out from the shot point and these gradients define apparent velocities of the propagating waves. There is a high degree of symmetry in the behaviour about the shot point. Standard seismic refraction analysis of the first arrivals indicates a three layer velocity sequence of 180, 380 and 1000 m/s with interface depths of 0.6 and 1.3 m. Although there are indications of superimposed effects following the first arrival (first negative/positive going pulse), two further arrivals (> 40 ms) arrivals can be identified having estimated moveout velocities of 400 and 1300 m/s. These velocities are consistent with head waves propagating along the two refractor interfaces.

The voltage data, colour-contoured in the right frame of Figure 6.11, appear to reflect the behaviour of the seismic data to some degree. The apparent move out velocity of the first three coherent oscillations (at times > 20 ms) is about 325 m/s and they possess the same dominant frequency (about 90 Hz) as the seismic source. At times in excess of 5 ms, all the voltage oscillations appear to be associated with EK coupling due to the passage of horizontally propagating acoustic waves. At times < 5 ms, however, a high frequency oscillation (positive/negative/positive) is observed simultaneously across the dipole spread. Converting the onset time of the signal (2.5 ms) to depth, assuming an upper layer velocity of 180 m/s, yields a depth of 45 cm. This depth is in close agreement with the observed water level in pits dug in the river bed and may therefore be interpreted as electrokinetic coupling at the water table.

The above example is one of the few where EK voltage returns appear simultaneously across arrays of surface dipoles. The shot-symmetric voltage returns that are typically observed in the vicinity of the shot point (having amplitudes in the millivolt range) appear to be commonly associated with the at and near-surface horizontal propagation of a variety of seismic waves.

6.4) Case study 4. Dartmoor granite.

Seismic refraction and electrokinetic measurements were conducted on the Dartmoor granite near the village of Postbridge. The electrokinetic measurements were the first profile measurements to be acquired using the high-resolution BGS TEKA system. Three closely spaced boreholes had been drilled in the attempt to locate a thickness of weathered granite suitable for directional drilling trials. These all proved 'fresh' granite at shallow depths (between 2.5 m and 3.9 m) and the hydrogeological condition can be assumed to be 'tight'. Our experiments were made along the 100 m profile linking boreholes 1 and 2.

The Postbridge refraction survey produced a seismic velocity cross-section along a 100 m profile

between two of the shallow boreholes. The velocity 'layering' is non-horizontal. The only uniform feature is the at-surface low velocity layer (150-200 m/s) of thickness 1 to 1.5 m. At the northern-most borehole, the estimated depth to 'intact' (velocity > 4000 m/s) granite is over 20 m. At the southern-end of the profile moderate velocities (2700 m/s) indicate fairly weathered granite at shallow depth (1.5 m). The picture at the site is one of a concealed granitic 'boss' previously outcropping to the south of the survey line. Above the intact granite (and shelving in a similar fashion) two velocity zones are observed. The upper zone has velocities < 1000 m/s and the lower zone has velocities in excess of 1000 m/s (typically 1500 m/s). **Clearly this seismic interpretation is at variance with the drilling results described above.**

The 100 m profile of EK measurements followed the refraction profile between the shallow boreholes. Two-channel sounding centres were positioned at 5 m intervals using the standard arrangement of 2 m dipoles and a sampling interval of 10 kHz. Unexpectedly the data set obtained was of relatively high amplitude and showed evidence of voltage coupling to far later times (apparent depths) than had been observed anywhere previously.

Figure 6.12 shows the data obtained at 25 m with the upper frame displaying the first 200 ms of data and the lower frame showing the second 200 ms of data using a reduced amplitude scale. The persistence of in-phase behaviour is remarkable; even through the second 200 ms interval, where low frequency oscillations dominate, the 2 channels display in-phase behaviour. A less persistent recording made at 70 m is shown in Figure 6.13. Here, in-phase behaviour persists to about 120 ms and at later-times the data revert to anti-phase noise residuals.

The 2-channel profile data obtained across the profile are summarised in Figures 6.14 and 6.15. The data are trace normalised and colour-contoured to image the main features of the voltage oscillations. In Figure 6.14, the first 100 ms of the data are shown and over the first 20 ms a high degree of lateral continuity exists. At later times the lateral continuity tends to disperse. The main feature, however, is the high degree of in-phase behaviour exhibited by the two channels both spatially and in time. This in-phase behaviour is seen to persist to 200 ms in Figure 6.15, where although voltage amplitudes have decayed to the microvolt level (Figures 6.12 and 6.13), and more noise is evident, the main voltage oscillations are reproduced in the two channels.

The spatial and temporal characteristics observed indicate a shallow origin for the coupling. Interfaces generating the in-phase coupling over the first 20-30 ms are relatively, though not entirely, uniform across the 100 m profile. With increasing time, the in-phase behaviour is maintained but the specific form of the voltage oscillations is increasingly localised to about the same scale as the measurement array (i.e. 5 m). It is clearly conceptually difficult to equate the later time coupling to increasingly deep and 'spatially localised' interfaces within the intact granite at depths greater than 20 m. The interpretation of the data characteristics is that all the coupling observed is generated in the near-surface (i.e. depths less than 20 m).

If one of the soundings were interpreted following the methodology of the commercial system, the results would imply the granite site was a major multi-story aquifer. Due to the high velocities at the site, the depths estimated on the assumption of a vertical coupling model would extend to many hundreds of metres. The data set was critical in providing evidence for the flaws in the stated methodologies.

7) SUMMARY

This study has brought together theory and field studies to assess the relevance of electrokinetic sounding to well and borehole siting in diverse hydrogeological environments. The starting point of the assessments was the instrument and procedures of a new geophysical methodology brought to the marketplace by a new company. Our assessments have, of necessity, been scientifically critical. It is acknowledged that subsurface EK coupling can be routinely observed, however, it is the interpretation of the data that has been a key issue of the study. An important element in our assessment is the set of **'simplifying assumptions'** that are embodied in the proposed method.

The theory and concepts underpinning geophysical observations of electrokinetic coupling have been reviewed. It is acknowledged that both concepts and theory are still developing and the procedures adopted may be an important 'first-step'. Both theory and experiment have confirmed that, in the limiting case of two channel operation, the use of 2 m dipoles centred at 1.5 m from the shot point is generally optimum for 'signal' detection and noise rejection.

The simplifying assumptions behind the proposed methodology are :

- The water table can be identified from the raw 2-channel data.

Numerous data sets display in-phase behaviour from very early times (a few milliseconds). This is anticipated in situations where the water table is shallow; however the behaviour is often repeated in situations where the water table is deep (tens of metres). Large amplitude voltage responses are clearly generated in the vadose zone. Theory predicts that a change in streaming potential coefficient can generate EK coupling. The coefficient depends on both pore fluid properties (e.g. air or water, the degree of saturation and fluid electrical conductivity) and the microstructural rock properties (e.g. porosity and permeability).
Given this complex level of dependency the 'simple' detection of the water-table using the methodology does not appear justified either by theory or by the experimental results presented.

- the voltage returns observed by two symmetrical surface dipoles can be interpreted entirely by Fresnel zone coupling vertically beneath the shot point.

Both theory and the extended field experiments described here and by others (Butler et al., 1997; Mikhailov et al., 1997) indicate that this is an invalid assumption. By far the most common feature of the recordings are voltages which possess spatial moveout and are therefore associated with horizontally propagating wave components.

■ Theory predicts that EK coupling due to vertical wave propagation will produce 'simultaneous' arrivals across an array of surface dipoles.

This is the most significant characteristic of the assumption. The use of only two channels does not provide any confirmation that this required procedural assumption is upheld. All but one of our extended, multi-channel experiments have failed to detect this characteristic.

■ Voltage rise-times can be used to estimate porosity/permeability.

As the manufacturers acknowledge, this is an ambitious procedure. In our opinion, the rise-time of the EK voltage recordings are, primarily, determined by the form of the acoustic source rather than being a measure of permeability. Following on from this, the estimation of hydrogeological parameters of an aquifer (part of the methodology) which is based on the use of voltage rise-time appears to be a highly questionable exercise.

The methodology proposed by the manufacturers has been described here as a 'limiting (2-channel) case' of a wider (multi-channel) assessment of electrokinetic field behaviour. The first assumption of the proposed methodology is that 2-channel recording is sufficient to describe the EK coupling at the site. The extended multi-channel experiments have deliberately included the position of the standard two-channel sounding configuration and extended the observations inwards (towards the shot point) and outwards (away from the shot point). The hydrogeological environments tested range from the extreme (clays and granites) to the routine sandstone aquifers both in the UK and overseas. These include 'tight' situations (clays and shallow 'fresh' granites) and, conversely, highly porous/permeable sand rivers and consolidated sandstone (a major aquifer) displaying, respectively, shallow and deep water tables. In every case numerous early time EK signals showing moveout have been observed. By implication the main generation mechanism appears to be due to coupling along interfaces by horizontally propagating acoustic waves.

An important general result of the moveout experiments has been the apparent slow velocities detected. This has been persistently observed despite the fact that the large scale refraction experiments at the test sites have identified the expected transitions from low to high acoustic velocities with increasing depth. For the experimental voltage data shown in the near-vicinity of the shot-point (+/- 5 m) the apparent wave velocities do not exceed 500 m/s. Typically they are much lower and velocities as low as 120 m/s have been observed. Again in the near-vicinity of the shot point the joint acoustic data indicate similar low moveout velocities. The implication, both from the scale of the experiments and the velocities obtained is that both sets of waves are associated with propagation in the very near surface, highly unconsolidated material.

At the present time there is a paucity of firm theoretical predictions concerning the complete

nature of EK coupling. These are required to add substance to the interpretation of the extended experimental observations presented here. The main predictions that are available concern the roles of vertical (P-wave) and horizontal (refracted head wave, etc.) effects, as discussed previously.

The main lack of predictions concern the role of EK coupling along the free surface (meaning the role of the horizontally propagating direct and Raleigh waves) which are likely to be highly significant. Butler et al. (1997) discuss anticipated direct P-wave effects but no publications have dealt with the slower surface wave effects. According to Pride (1997, personal communication) there should be a very large E-field inside a surface wave (the boundary being the free surface) that would be recorded as the wave passes surface dipole antennas. The 'picture' is one of an expanding circular wave-front creating a vertical mismatch in streaming potential current (due to the interface) which would act as a circular region of vertical dipoles. Although the low moveout velocities of much of our voltage data are compatible with the slow acoustic propagation of Rayleigh and direct waves, the expectation is that such waves would trace back to time zero at the shot point location. This behaviour is not observed. The moveout behaviour observed appears to be more readily interpreted by horizontally propagating refracted head wave effects.

In final summary it is suggested that the theoretical and experimental results presented here indicate that some important assumptions of the proposed methodology are flawed. A vertical sounding capability has not been established. The routine use of the equipment and the modus operandi established in the manual is likely to :

- provide insufficient information into the nature of EK coupling at the site, and
- provide a false interpretation under the assumptions stated in the manual.

8) THE WAY FORWARD

The results of the study provide some very clear indicators as to the way forward. At present electrokinetic coupling in the shallow subsurface appears to be routinely observed. The information relates to zones of high fluid mobility and/or large fluid chemistry contrasts (rather than the water table *per se*). Interpretation is both speculative (limited theoretical predictions) and complex (e.g. akin to a seismic refraction experiment).

In the context of increasing the success rate of well siting it is necessary to be pragmatic. In our opinion the current state of electrokinetic sounding is sufficiently research-based to rule-out a simple use for increasing the success rate of well and borehole siting.

For 'simple' applied hydrogeological purposes it would be necessary to investigate the detection of deeper interfaces by isolating the vertical sounding components of coupling from within the

complex patterns that the acoustic source generates. The prognosis is that this would be a difficult task due to the decreasing signal amplitude with depth. The extent to which such a method could be routinely applied requires research.
As noted above, the objective would be to provide a methodology that confirms and then exploits the vertical sounding capability of electrokinetic coupling. The characteristic to be exploited concerns the recording and identification of simultaneous arrivals across an array of surface dipoles. The signal amplitudes are predicted to decay rapidly away from the shot point location. Predicted amplitudes also decay rapidly with increasing depth. These facts imply a requirement for acquisition systems with a high fidelity and dynamic range. Advanced geophysical signal processing methodologies might also be required to extract small signals embedded in noise. The type of methodology described conforms to that of a modern, high resolution seismic acquisition system, but perhaps with fewer channels. One step along this route is provided by the BGS TEKA system which is being used to carry out research and development. At this stage it should be noted that, even with a high level of sophistication in place, the information content might not relate 'simply' (i.e. without modelling and data inversion) to simple assessments of the water table.

In the wider context of geophysical assessments for well-siting, electrokinetics is unique in that it has the capability of providing **direct** information on zones of high permeability. The fact that the signal may also be generated by fluid chemistry contrasts and different layers of microstructural fabric throughout both vadose and saturated zones are complicating factors. At present geophysical assessments of hydrogeology, especially overseas, use tools which provide measures of the subsurface resistivity distribution. The methods involve both electrical and electromagnetic techniques. Different hydrogeological problems and different required depths of investigation may require decisions about the most appropriate methodology. The bulk resistivity will remain a largely **indirect** measure of hydrogeologically useful parameters. This simply means that an element of sophistication and coordination between hydrogeologist and geophysicist must remain part of the picture if useful and more-certain information is to be routinely extracted.

Tried-and-tested resistivity techniques remain the backbone of overseas geophysical assessments. It is worth noting that technology and methodologies continue to evolve with trends evident in both (i) increasing sophistication and (ii) operator/interpreter user-friendliness. The combination can provide for highly-effective tools. Many of the modern electrical and electromagnetic techniques are profiling methods which deliver depth cross-sections of the resistivity structure in some detail. Such two-dimensional cross-sections assist with the separation of the structural components (in the vicinity of a target location) and the specific vertical resistivity distribution at a target location. There is a cost/benefit analysis to be undertaken in the routine use of geophysical assessments for well-siting however there is no doubt that with primary/easier targets disappearing, the prognosis is for the use of more sophistication to assist with maintaining/increasing success rates.

9) REFERENCES

Ahmed, M.U., 1964. A laboratory study of streaming potentials. Geophys. Prosp., 12, 49-64.

Beamish, D., Peart, R.J. and Davies, J, ...1997. Electrokinetic measurements in various hydrogeological environments of Zimbabwe. British Geological Survey Technical Report **WC/97/31.** A report prepared for the O.D.A.

Biot, M.A., 1956. Theory of propagation of elastic waves in a fluid saturated porous solid, I. Low-frequency range. J. Acoust. Soc. Am., 28, 168-178.

Biot, M.A., 1962. Mechanics of deformation and acoustic propagation in porous media. J. Appl. Phys., 33, 1482-1498.

Bockris, J. And Reddy, A.K.N., 1970. Modern Electrochemistry. Plenum Press.

Broding, R.A., Buchanan, S.D. and Hearn, D.P., 1963. Field experiments on the electroseismic effect. IEEE Trans. Geoscience Electronics., GE-1, 23-31.

Butler, K.A., Russell, R.D., Kepic, A.W. and Maxwell, M., 1997. Measurement of the seismoelectric response from a shallow boundary. Geophysics, 61, 1769-1778.

Chandler, R.N., 1981. Transient streaming potential measurements on fluid-saturated porous structures : an experimental verification of Biot's slow wave in the quasi-static limit. J. Acoust. Soc. Am., 70, 116-121.

Corwin, R.F. and Hoover, D.B., 1979. The self-potential method in geothermal exploration. Geophysics, 44, 226-245.

Debye, P., 1933. A method for the determination of the mass of electrolyte ions. J. Chem. Phys., 1, 13.

Dietrich, M., Garambois, S. and Glangeaud, F., 1996. Seismo-electric effects : a field example over a shallow aquifer. Proc. EEGS 2nd Annual Meeting, Nantes, France, 1996, 82-84.

Dobrin, M.B. and Savit, C.H., 1988. Introduction to Geophysical Prospecting. McGraw-Hill Book Co., N.Y.

Fitterman, D.V., 1978. Electrokinetic and magnetic anomalies associated with dilatant regions in a layered earth. J. Geophys. Res., 83, 5923-5928.

Ishido, T. And Mizutani, H., 1981. Experimental and theoretical basis of electrokinetic phenomena in rock-water systems and its applications to geophysics. J. Geophys. Res., 86, 1763-1775.

Ivanov, A.G., 1939. Effect of electrization of earth layers by elastic waves passing through them (in Russian). Doklady Akademii Nauk SSSR, 24, No. 1., 41-45.

Jouniaux, L. And Pozzi, J.P., 1995. Permeability dependence of streaming potential in rocks for various fluid conductivities. Geophys. Res. Lett., 22, 485-488.

Lageman, R., Pool, W. and Seffinga, G., 1989. Electro-reclamation theory and practice. Chem. Ind. London, 18, 575-579.

Long, L.T. and Rivers, W.K., 1975. Field measurement of the electroseismic response. Geophysics, 40, 233-245.

Martner, S.T. and Sparks, N.R., 1959. The electroseismic effect. Geophysics, 24, 297-308.

Milkhailov, O.V., Haartsen, M.W. and Toksoz, M.N., 1997. Electroseismic investigation of the shallow subsurface : Field measurements and numerical modeling. Geophysics, 62, 97-105.

Millar, J.W.A. and Clarke, R.H., 1995. The application of electrokinetic surveying to mining. Report to MIRO members (Ref. IC 110).

Mizutani, H.T., Ishido, T., Yokokura, T. And Ohnishi, S., 1976. Electrokinetic phenomena associated with earthquakes. Geophys. Res. Lett., 3, 365-368.

Murty, Y.S., 1985. First results on the direct detection of groundwater by seismoelectric effect - a field experiment. Bull. Austr. Soc. Expl. Geophys., 16, 254-255.

Neev, J. And Yeatts, F.R., 1989. Electrokinetic effects in fluid-saturated poroelastic media. Phys. Rev. B., 40, 9135-9141.

O'Brien, R.W., 1988. Electro-acoustic effects in a dilute suspension of spherical particles. J. Fluid Mech., 190, 71-86.

Overbeek, J.Th.G, 1952. Electrochemistry of the double layer. *Colloid Science*, Vol. 1, Irreversible Systems, Ed. H.R. Kruyt, Elsevier, New York, 115-193.

Parkhomenko, E.I., 1971. Electrification phenomena in rocks. Plenum Press.

Parkhomenko, E.I. and Gaskarov, I.V., 1971. Borehole and laboratory studies of the seismoelectric effect of the second kind in rocks. Izv. Acad. Sci. USSR, Physics of the Solid Earth, 9, 663-666.

Peart, R.J., Davies, J. and Beamish, D., ...1995. Trial surveys with the electrokinetic survey technique in the Red River Basin, Vietnam. British Geological Survey Technical Report **WN/95/36**. A report prepared for the O.D.A.

Peart, R.J., Beamish, D., and Mathew, B, ...1997a .Well and borehole siting by Electrokinetic sounding and associated experimental observations in Bikita District, southern Zimbabwe. British Geological Survey Technical Report **WC/97/02.** A report prepared for the O.D.A.

Peart, R.J., Beamish, D., and Davies, J, ...1997b. Electrokinetic measurements in various hydrogeological environments of Egypt. British Geological Survey Technical Report **WC/97/32.** A report prepared for the O.D.A.

Pride, S.R., 1994. Governing equations for the coupled electromagnetic and acoustics of porous media. Phys. Rev. B., 50, 15678-15696.

Pride, S.R. and Haartsen, M.W., 1996. Electroseismic wave properties. J. Acoust. Soc. Am., 100, 1301-1315.

Pride, S.R. and Morgan, F.D., 1991. Electrokinetic dissipation induced by seismic waves. Geophysics, 56, 914-925.

Revil, A., Darot, M. And Pezard, P.A., 1996. From surface electrical properties to spontaneous potentials in porous media. Surveys in Geophysics, 17, 331-346.
Ricker, N., 1953. The form and laws of propagation of seismic wavelets. Geophysics, 18, 10-40.

Thompson, R.R., 1936. The seismic-electric effect. Geophysics, 1, 327-335.

Thompson, A.H. and Gist, G.A., 1993. Geophysical applications of electrokinetic conversion. The Leading Edge, SEG, 12, 1169-1173.

10) ACKNOWLEDGEMENTS

We gratefully acknowledge the high level of support provided throughout the Project by our overseas collaborators:

Dr Fatma Attia (Director), Engineer Youssef George Youssef (Head of Dissemination) and their senior colleagues at Egypt's Research Institute for Ground Water, and

Messrs Sam Sunguro (Chief Hydrogeologist) and Lawrence Sengayi (Principal Hydrogeologist) of Zimbabwe's Department of Water Development. Also in Zimbabwe, we thank Messrs Robin Cadwallader (DFID, Harare) and Brian Mathew (of the Bikita Rural Water Supply and Sanitation Project) for their support for (and assistance during) the additional field testing in Bikita District.

In the UK, Phil Meldrum was largely responsible for constructing and refining the in-house multi-channel TEKA system while Peter Greenwood assisted with many of the field trials. Lastly we thank Jeff Davies of the Hydrogeology Group (Wallingford) for his major contribution to the overseas field work and his insights into the varied hydrogeological conditions.

This report summarises research funded by the United Kingdom Department for International Development (DFID), undertaken for the benefit of developing countries. The views expressed are not necessarily those of the DFID.

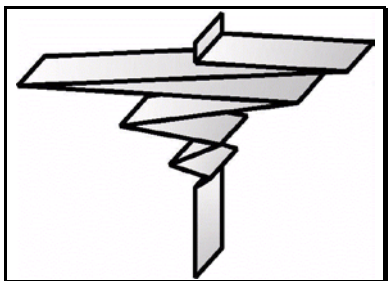

Fig. 4.1

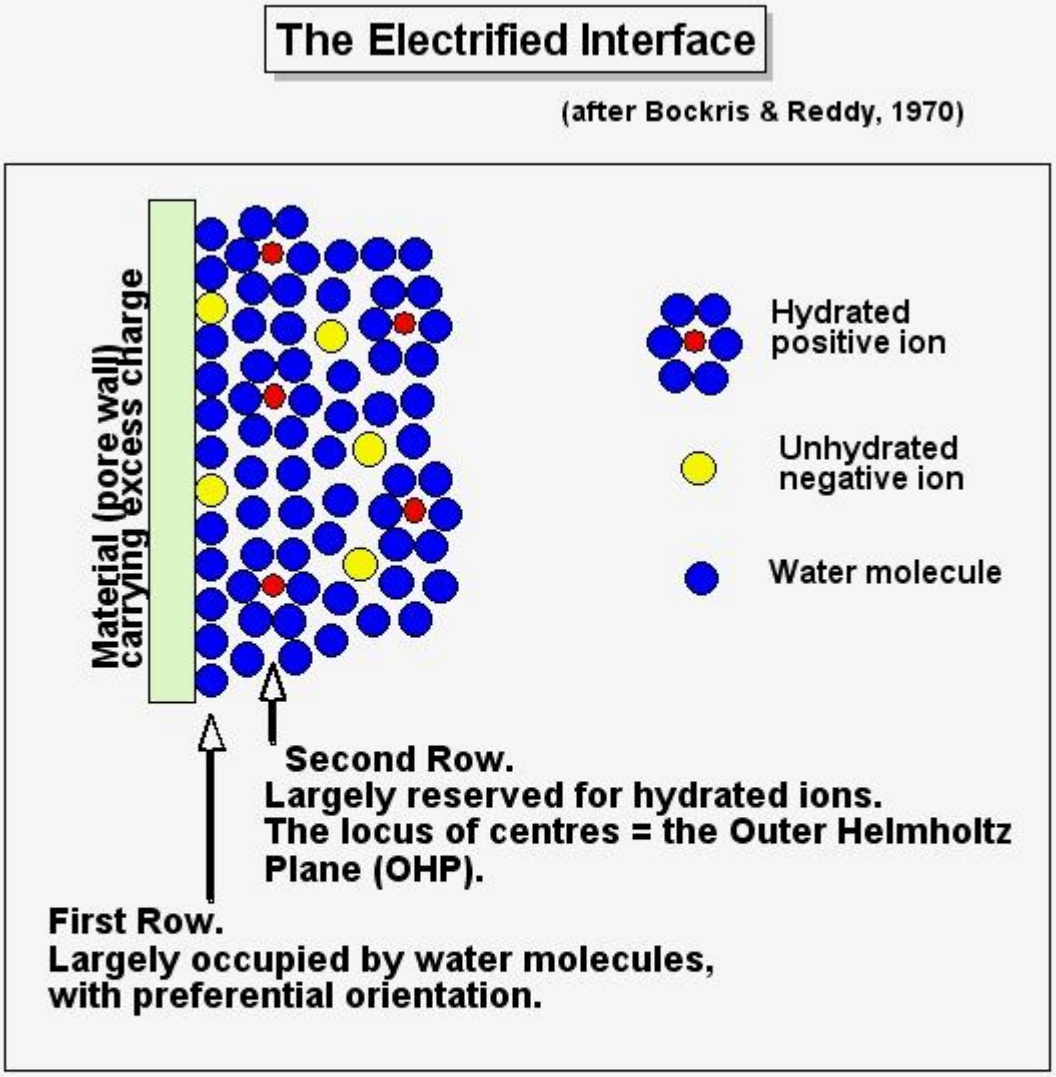

Figure 4.1. Schematic representation of the electrical double layer at a pore wall. In the simplest case, the excess charge density at the OHP is equal and opposite to that on the material. This situation, two layers of excess charge, gives rise to the term double layer

Fig. 4.2

The Electrified Interface

(after Bockris & Reddy, 1970)

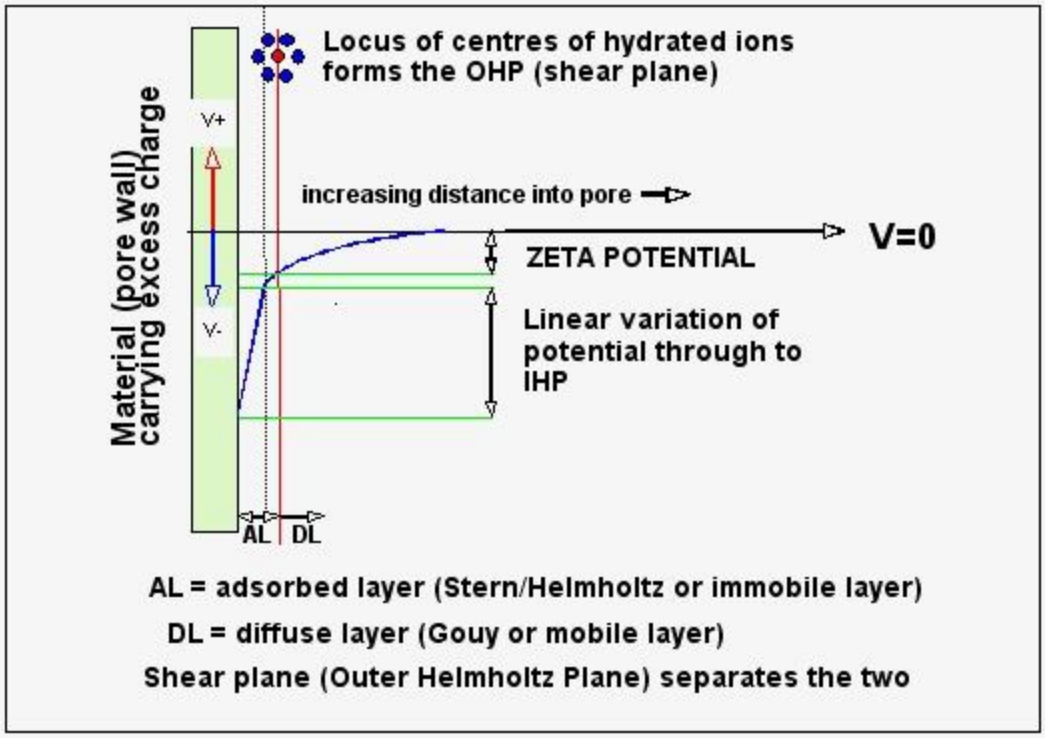

Figure 4.2. Schematic of the potential distribution across the electrical double layer.

Among many possible models of the electrical double layer, the Stern model, which has been improved by many authors is generally accepted (e.g. Overbeek, 1952).

The Stern (immobile) layer is, in general, divided into two layers called the Inner and Outer Helmholtz Planes (IHP and OHP).

Flow of pore fluid convects the DL producing a current flow (imbalance of the mobile ions). The charge separation sets up an electric field which causes a current through the pore fluid.

Fig. 4.3

Figure 4.3 Radius of first Fresnel zone.

Variation with depth in four materials from low to high acoustic velocity

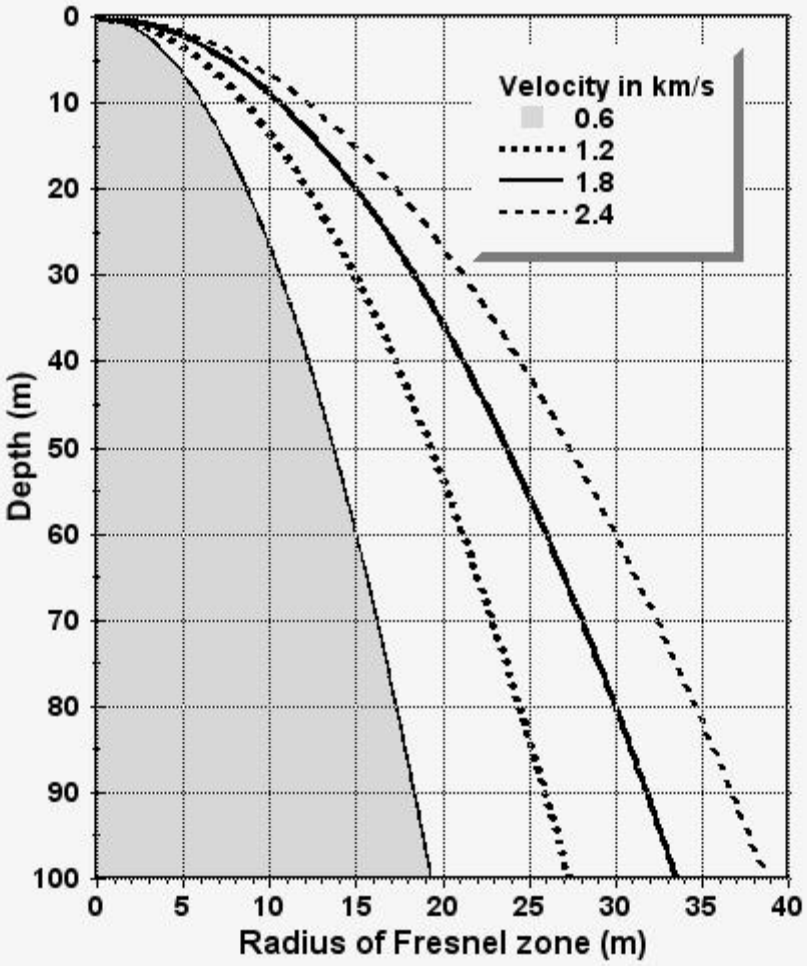

Source frequency=80 Hz. Uniform half-space

Source wavelengths (L) :

Vel.(km/s)	L (m)	L/4 (m)
0.6	7.5	1.9
1.2	15.0	3.7
1.8	22.5	5.6
2.4	30.0	7.5

Fig. 4.4

Figure 4.4 Theoretical Ricker wavelets

Frequencies of 500, 200 and 100 Hz

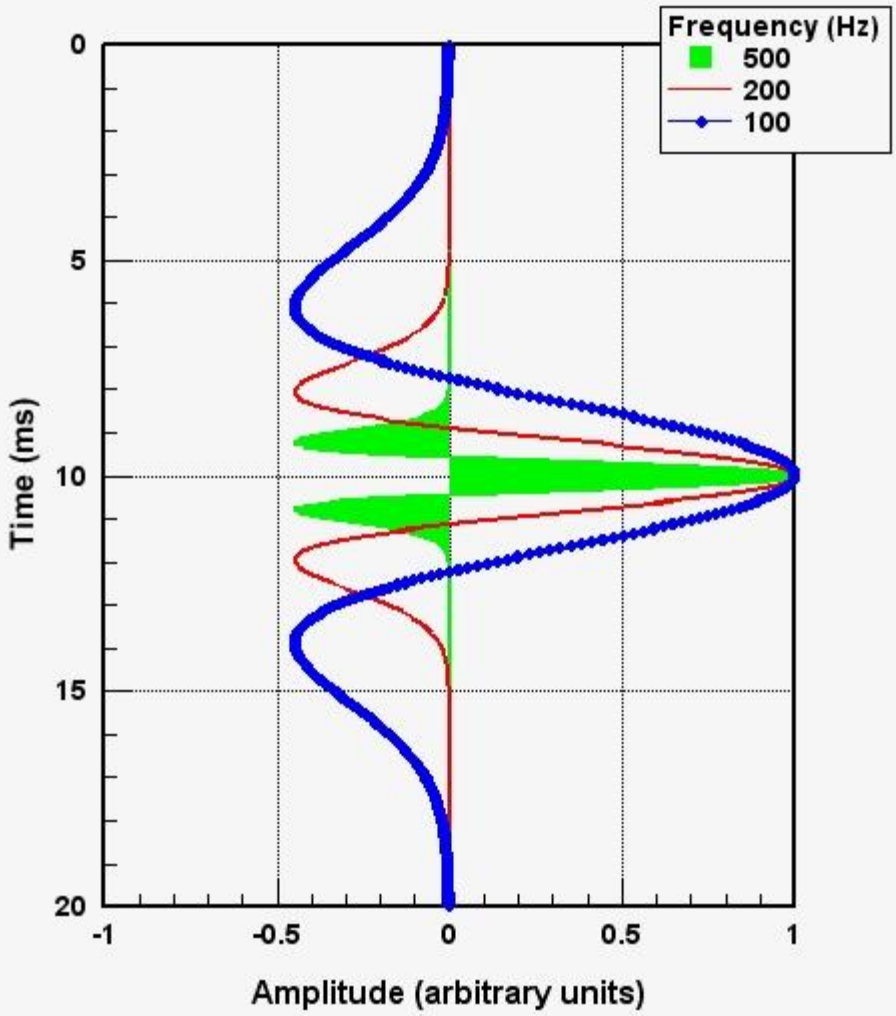

The wavelet has positive amplitude durations of :

0.90 ms (500 Hz)
2.25 ms (200 Hz)
4.50 ms (100 Hz)
9.00 ms (50 Hz)

Fig. 4.5

Figure 4.5 Schematic of the relative positions of various types of compressional seismic waves.

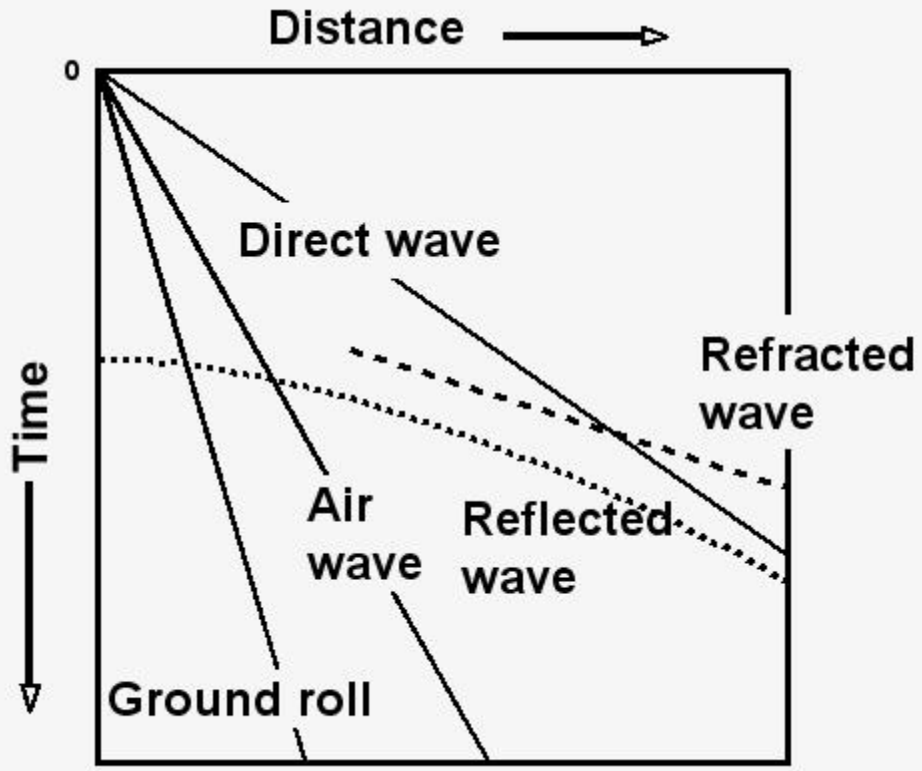

Fig. 4.6

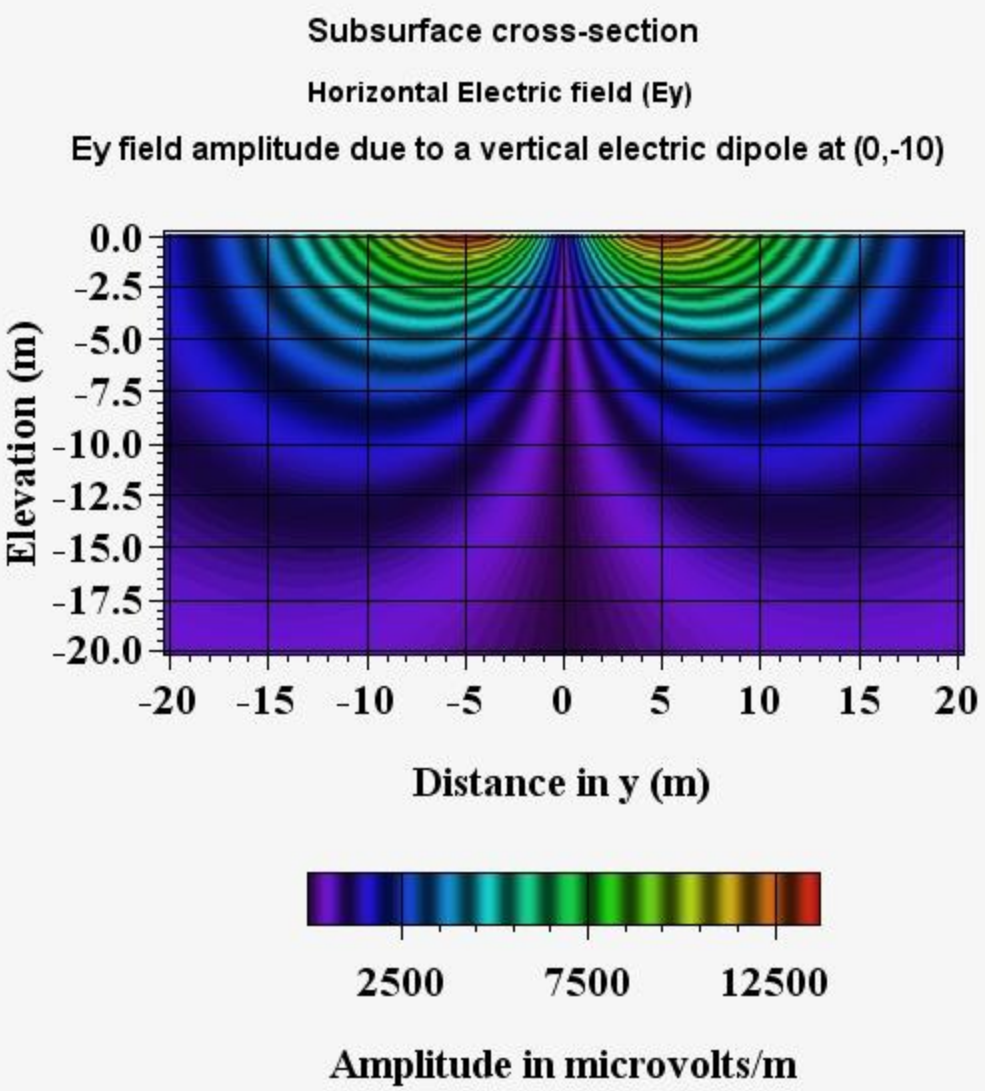

Figure 4.6. A subsurface cross-section showing contours of the amplitude of the horizontal electric field due to a vertical electric field dipole (VED) located at a depth of 10 m at y=0 m. The VED has unit dipole moment. The oscillation frequency is 80 Hz. The subsurface is uniform with a resistivity of 100 ohm.m and a dielectric constant of unity. The banded colour scheme emphasises the field gradients. A phase change of 180 degrees occurs about the plane of symmetry (y=0 m).

Fig. 4.7

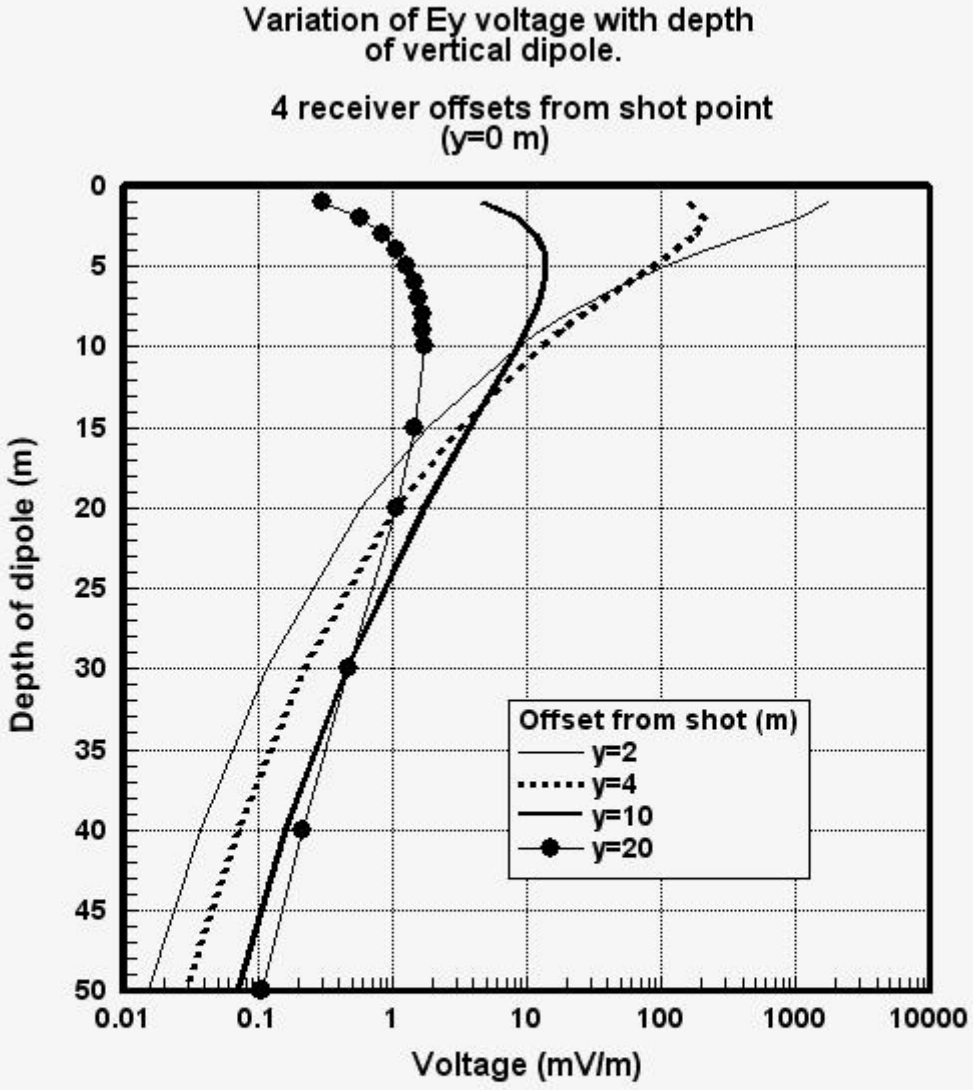

Figure 4.7 Variation of amplitude of horizontal electric field generated by a buried vertical electric dipole (VED) at depths from 1 to 50 m. Four measurement locations are shown at offsets of 2, 4, 10 and 20 m from the horizontal zero position of the buried dipole. The VED has a unit dipole moment at all depths. The oscillation frequency of the dipole is 80 Hz and the subsurface is uniform with a resistivity of 100 ohm.m and a dielectric constant of unity.

Fig. 4.8

Figure 4.8 **Results of synthetic EK modelling from Mikhailov et al. (1997). Upper frame = synthetic seismic data. Lower frame = synthetic electrical data.**

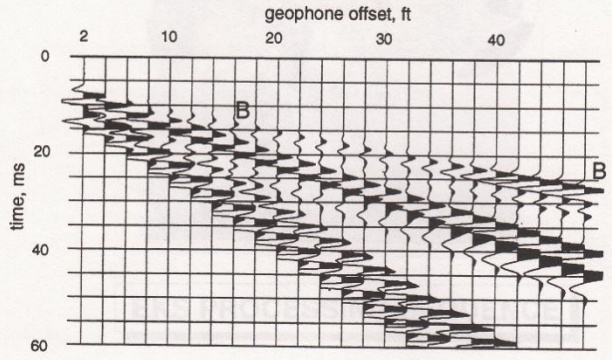

The synthetic seismic data. Event B-B is the refracted *P*-wave. Two later events are the refracted *S*-wave and the reflected *P*-wave.

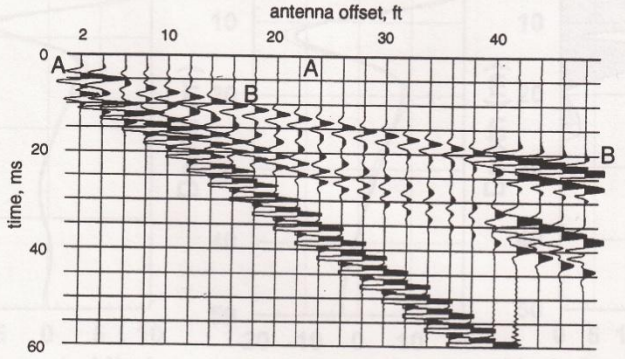

The synthetic electrical data. Event A-A is the electroseismic conversion at the interface. Event B-B is the electrical field generated by the head wave traveling along the interface. Two later events are due to electrical fields generated by the refracted *S*-wave and the reflected *P*-wave. In numerical calculations, we used a noncausal Ricker wavelet. Therefore we consider the time of a center peak as an arrival time, and the polarity of the center peak as the polarity of an electroseismic signal.

Figure 5.1 **Illustration of electrokinetic data acquisition and processing sequence**

EKS DATA ACQUISITION .

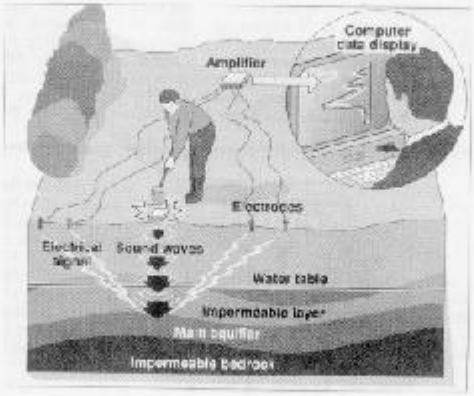

EKS PROCESSING SEQUENCE .

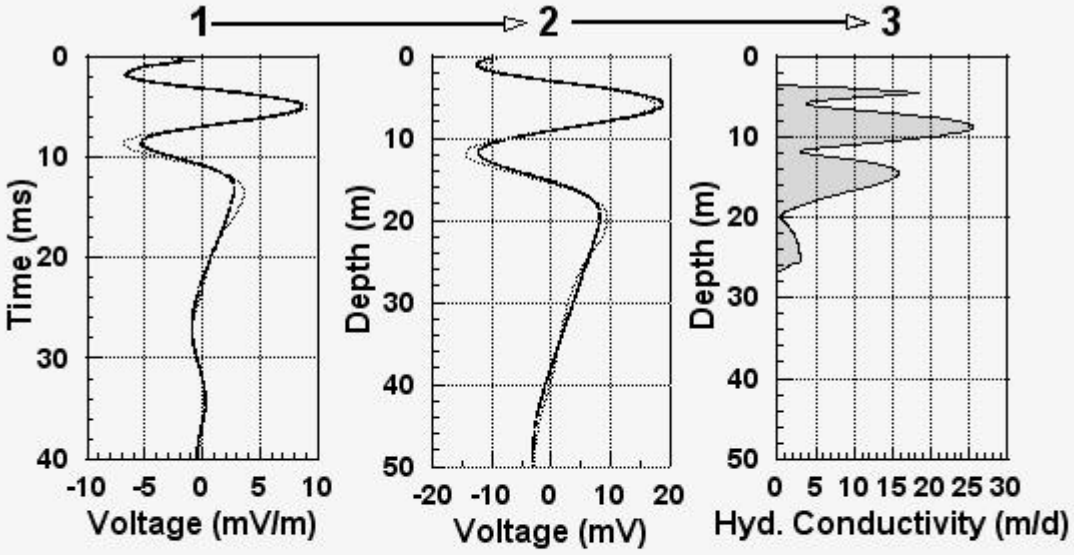

1) 2-channel voltage/time recording.

2) Time to depth conversion of voltages using a model of the acoustic velocity structure.

3) Voltage/depth converted to an estimate of permeability variation with depth.

Fig. 5.2

Figure 5.2 Example of EKS data repeatability
5 repeat shots - 2 data channels.
Orthogonal, same centre, soundings.

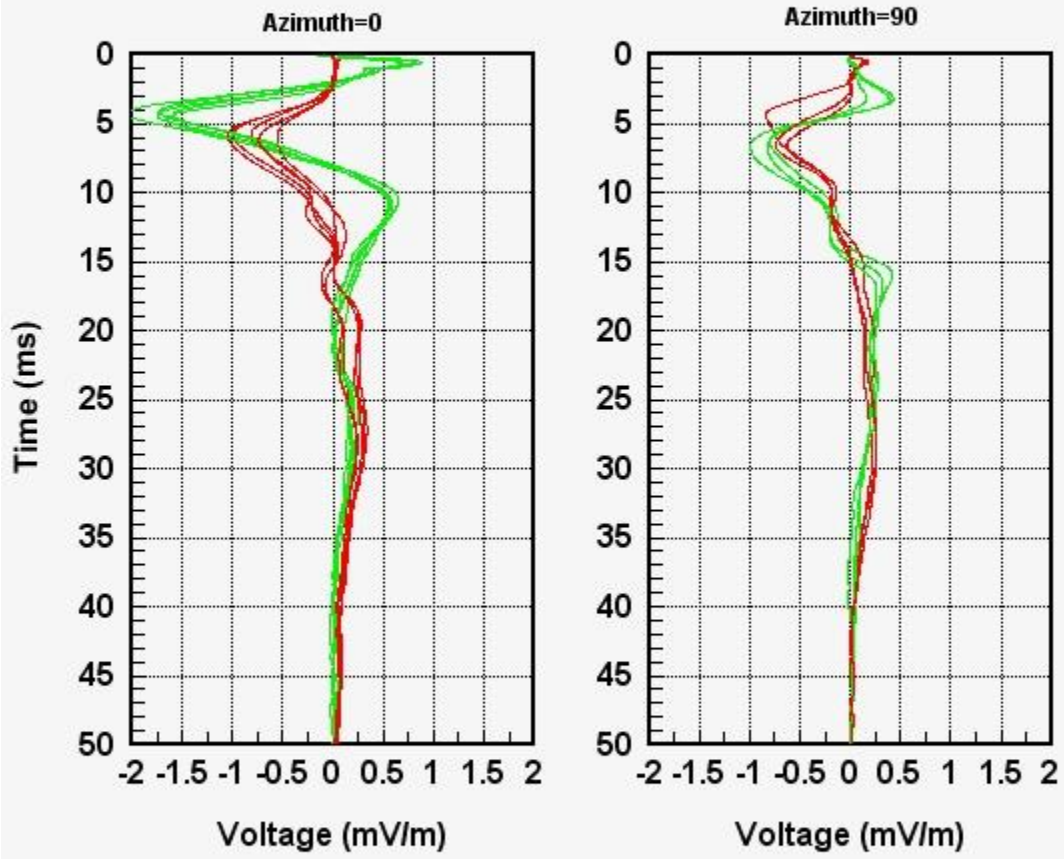

LOCATION : BH14, Save Valley, Zimbabwe.
SITE : BH14
Fluviatile sediments in graben.
Water level 9.5 m. Main supply 31 m, yielding
70-80 l/s, fresh.
Imains=0, Ifilt=1

Fig. 5.3

Figure 5.3
Overlay of 7 EK Soundings along a sand river profile.
Channel 1 (solid), channel 2 (broken line).
Cawood Ranch (CAW), Umzingwane River.
Fluviatile deposits over Karoo Basalt.

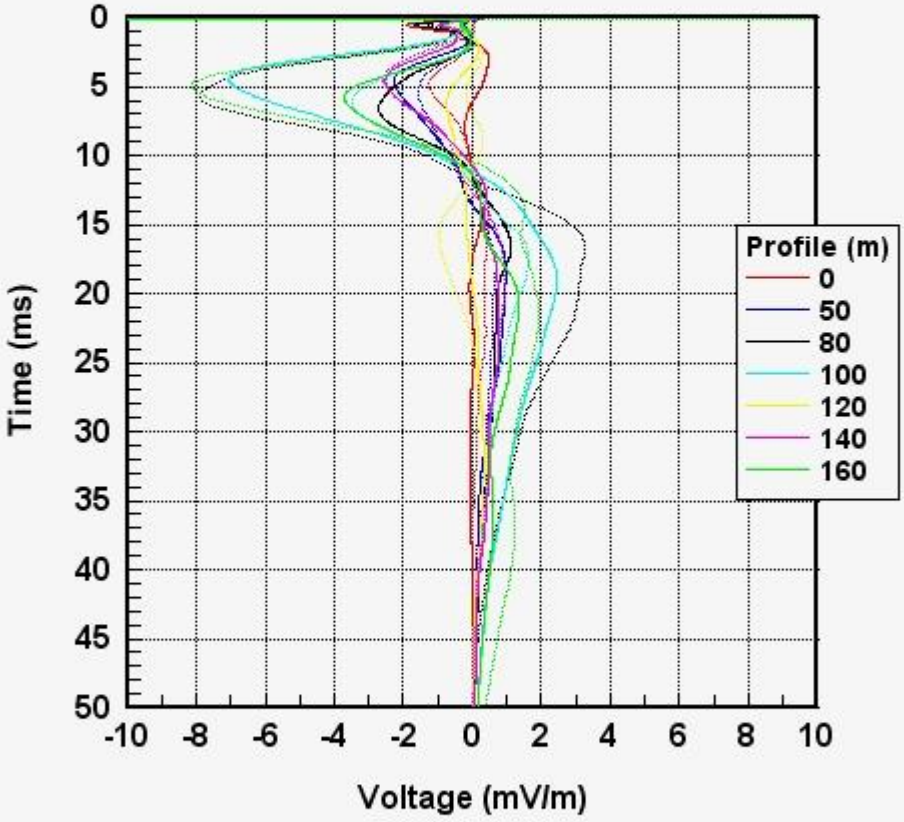

LOCATION : Cawood Ranch, Umzingwane Sand River, Zimbabwe.
SITES : NE [0, 50, 80, 100, 120, 140, 160 m] SW
Fluviatile sediments above Karoo Basalt.
0m (flank) is 6m above river.
Water table (BH) = 8 m, yielding 28 l/s from typically 17m depth.
Boreholes 3m apart display highly variable yields.
Imains=0, Ifilt=0

2-channel EK-sounding curves in Voltage/time.
Repeated sounding on two dates.
3 shots per sounding.

Fig. 5.4

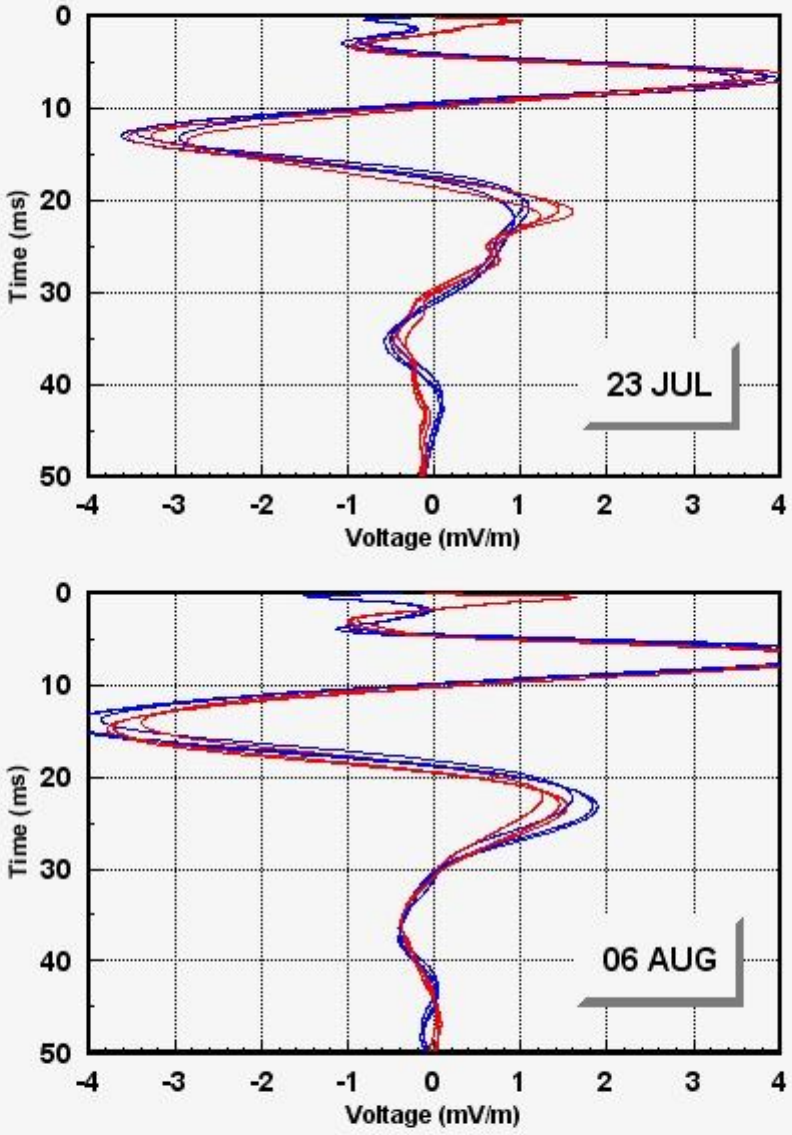

Figure 5.4. Typical shot-symmetric, two-channel (red and blue) sounding curves above a sandstone aquifer. The sandstone is capped by about 0.5 m of boulder clay. The water table is about 25 m deep.Data from three successive recordings (shots from a hammer/plate combination) are shown on each of two dates : 25 July 1996 (upper) and 6 August 1996 (lower). The experiment used dipole lengths of 2 m with the inner electrode positioned 0.5 m from the centre of the shot. The phase of one channel has been reversed such that a phase change of 180 degrees about the shot location would appear as in-phase behaviour on the two channels. The only digital processing applied is the removal of 50 Hz mains noise and associated harmonics.

Fig. 5.5

Figure 5.5 2-channel EK-sounding curves in Voltage/time.
Hall Farm Test Site Borehole
3 repeat shots shown

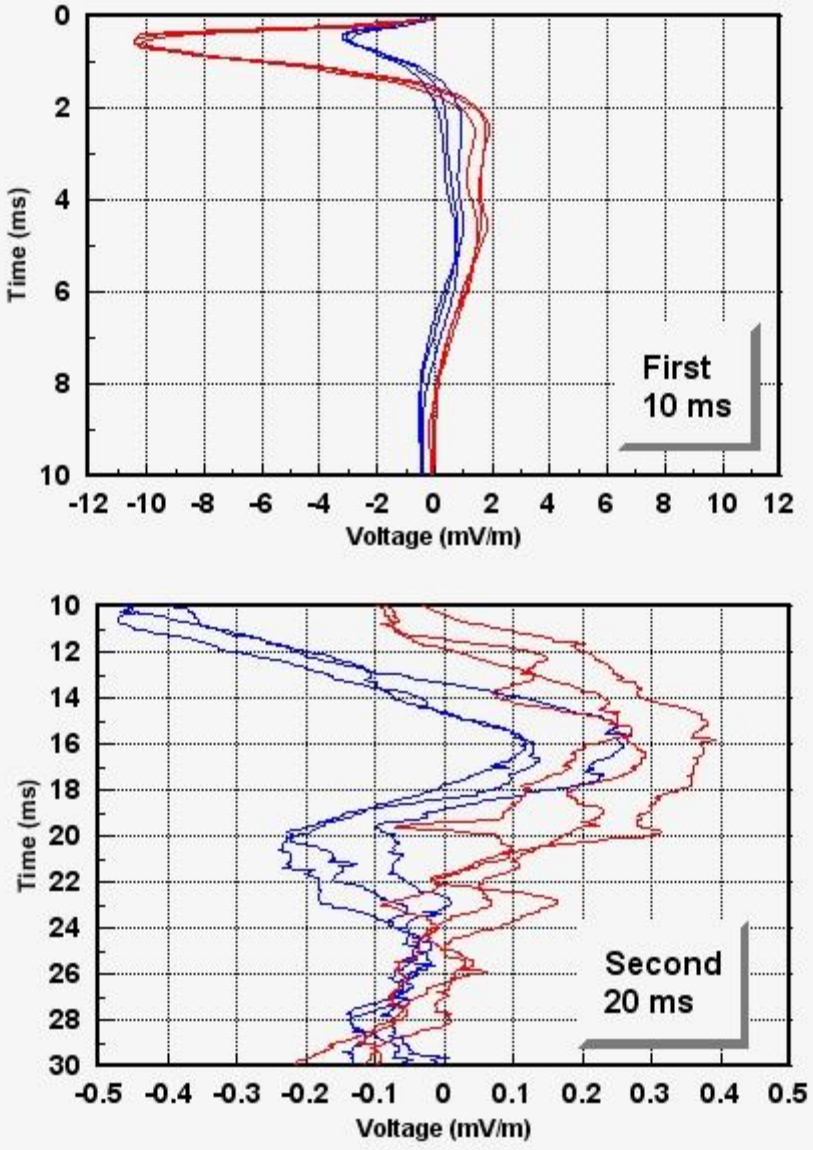

Figure 5.6 A comparison of field hydraulic conductivity results from in-situ hydraulic testing (symbols) and EKS sounding (infill). Hall Farm, East Anglia.

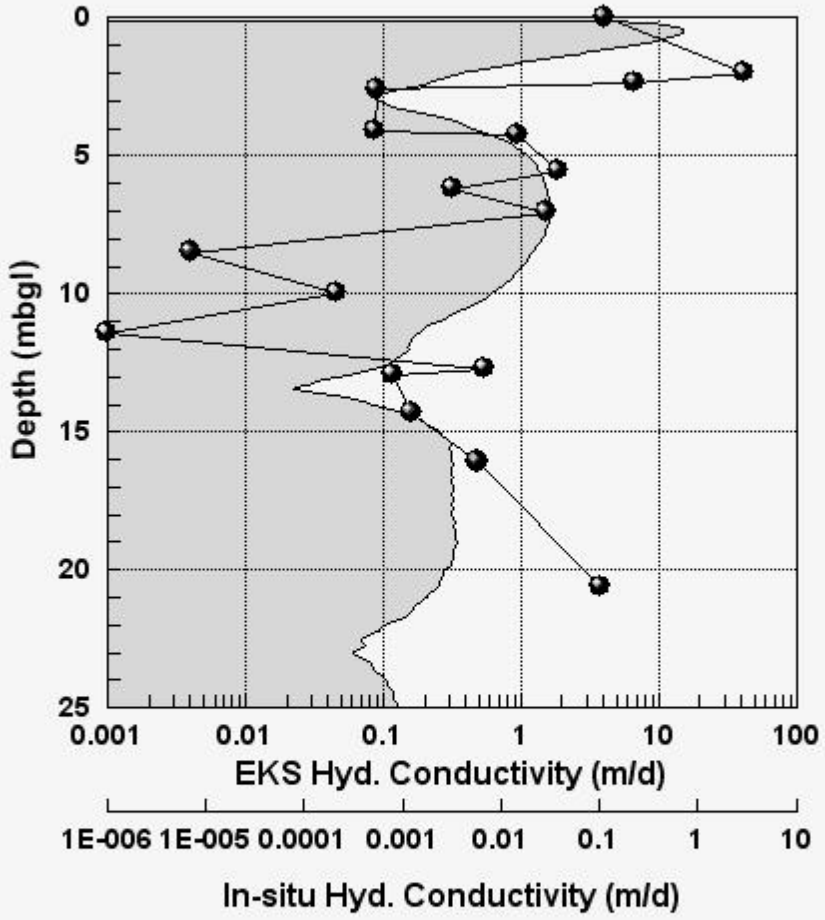

Site of test borehole. Sand to 2.25 m, clay sequence to 20.29 m above Chalk. Channel 1 result.

SITE	:GAR	Vel. 1 (m/ms)	:1.5
Watertable (m)	:0	Vel. 2 (m/ms)	:0.7
Base W.table	:100	Vel. 3 (m/ms)	:2.2
Chan.Hyd.Cond	:1	Depth v1/v2 (m)	:2
Porosity	:0.22	Depth v2/v3 (m)	:20

Fig. 5.7

Figure 5.7 2-channel EK-sounding curves in Voltage/time.
Two sets of adjacent (5m) soundings.
Typical Clay response (Note voltage scale).

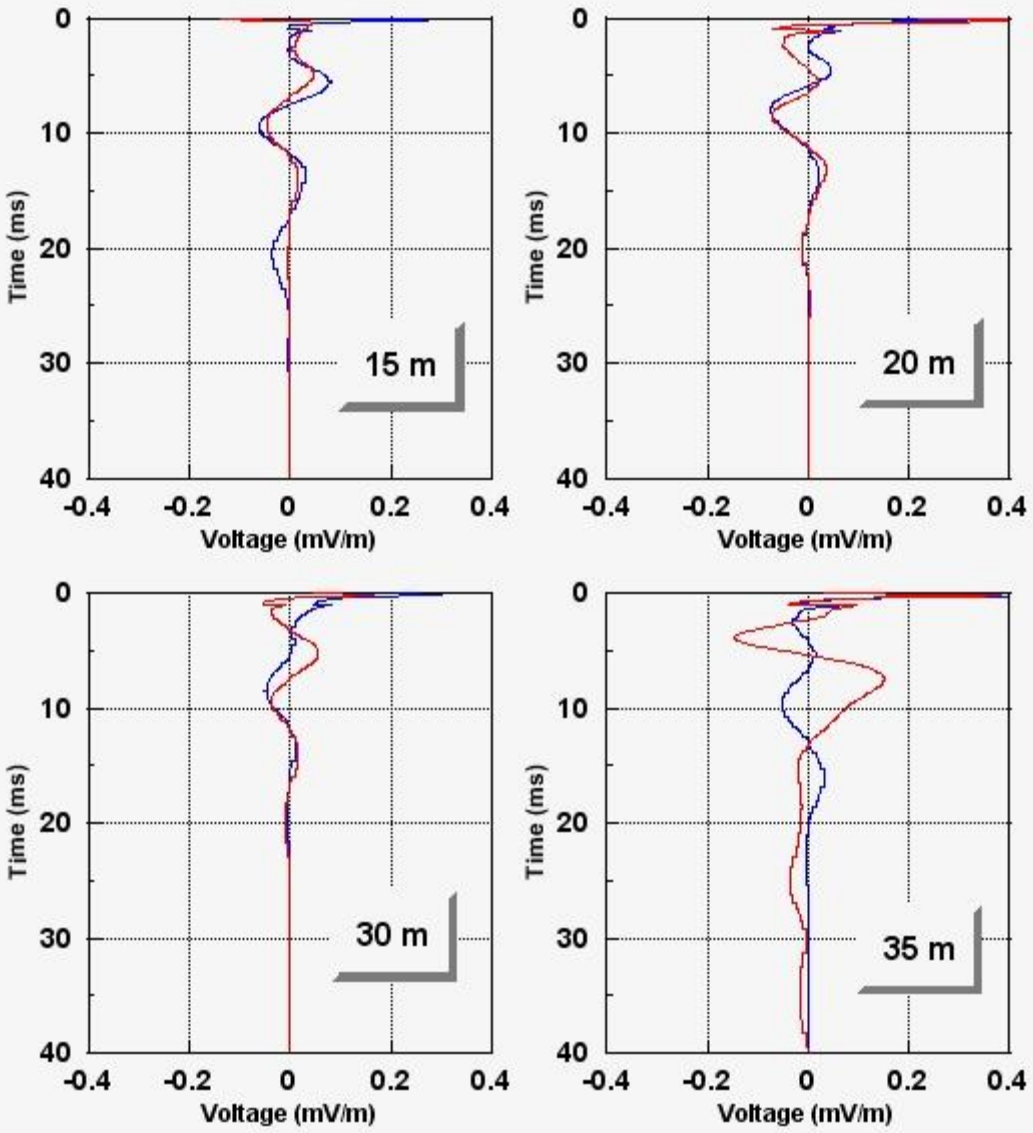

Scholes Farm/ CB BH. Positions 15,20,30,35m along profile
Geology : 40 m boulder clay on 150 m Lias clays/mudstones

Fig. 5.8

Figure 5.8 Colour-contoured EK voltage data along a profile. Channel 1 (upper) and channel 2 (lower)

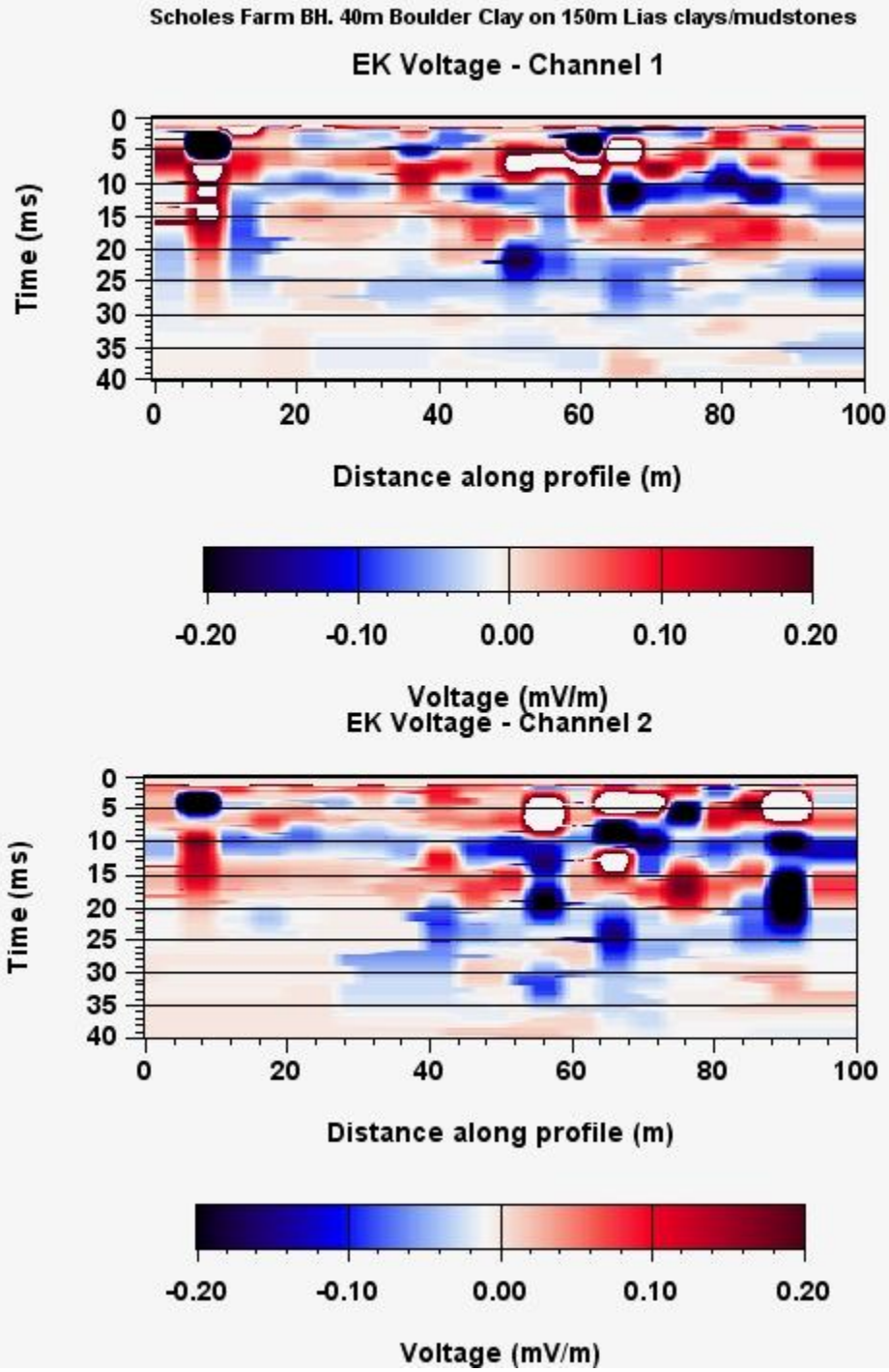

Figure 6.1 Schematics of (a) acoustic and (b) electrokinetic waves generated at a single interface

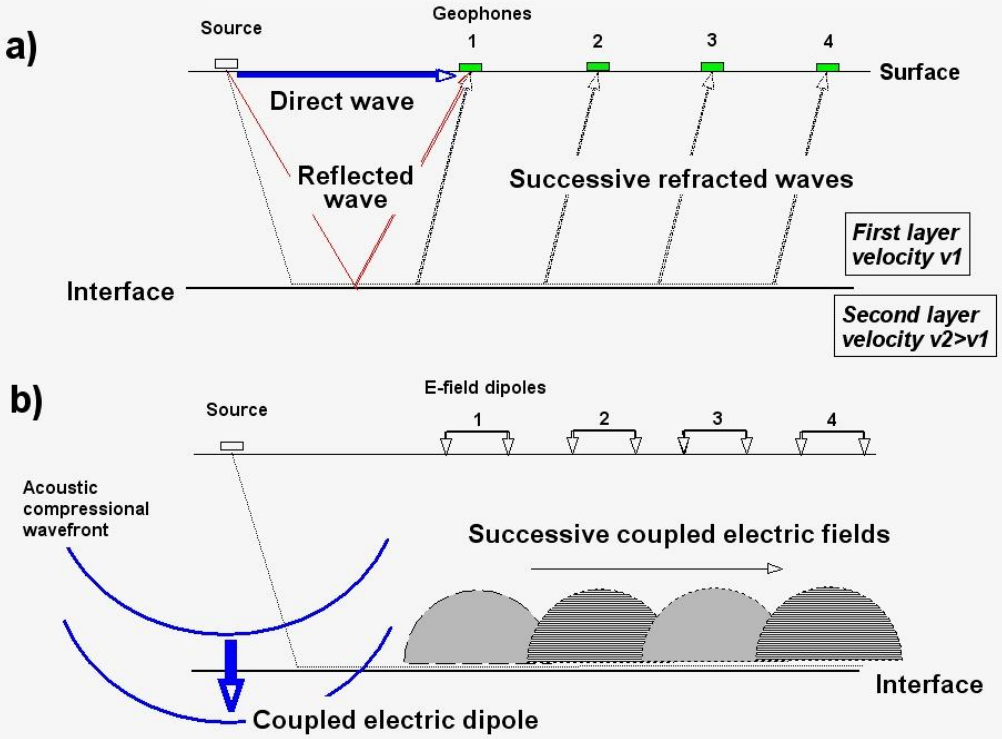

Fig. 6.1

Fig. 6.2

Figure 6.2 True voltage amplitudes for dipole lengths from 1 to 10 m, using same inner dipole at 0.5 m.

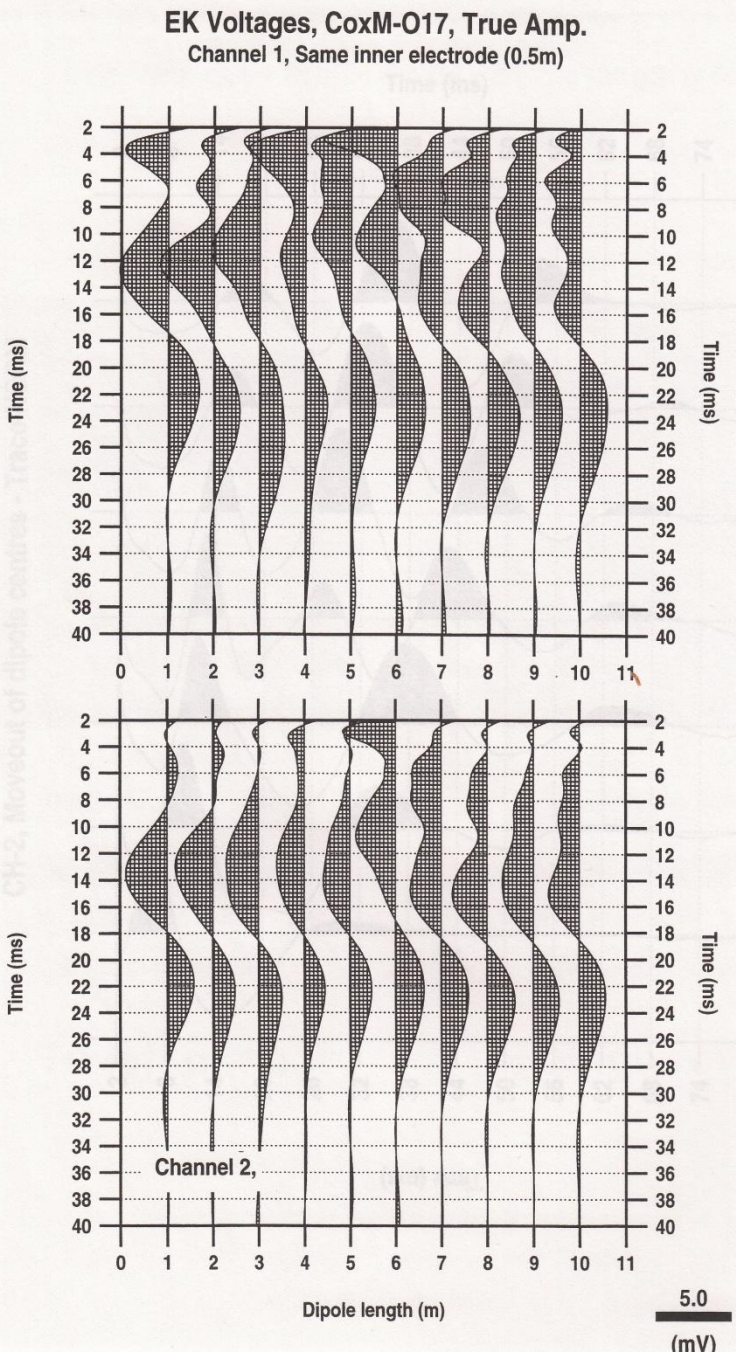

Fig. 6.3

Figure 6.3 Moveout experiment CoxM-N07. Dipole length = 0.5m. Channel 2 data, trace normalised (+/-)

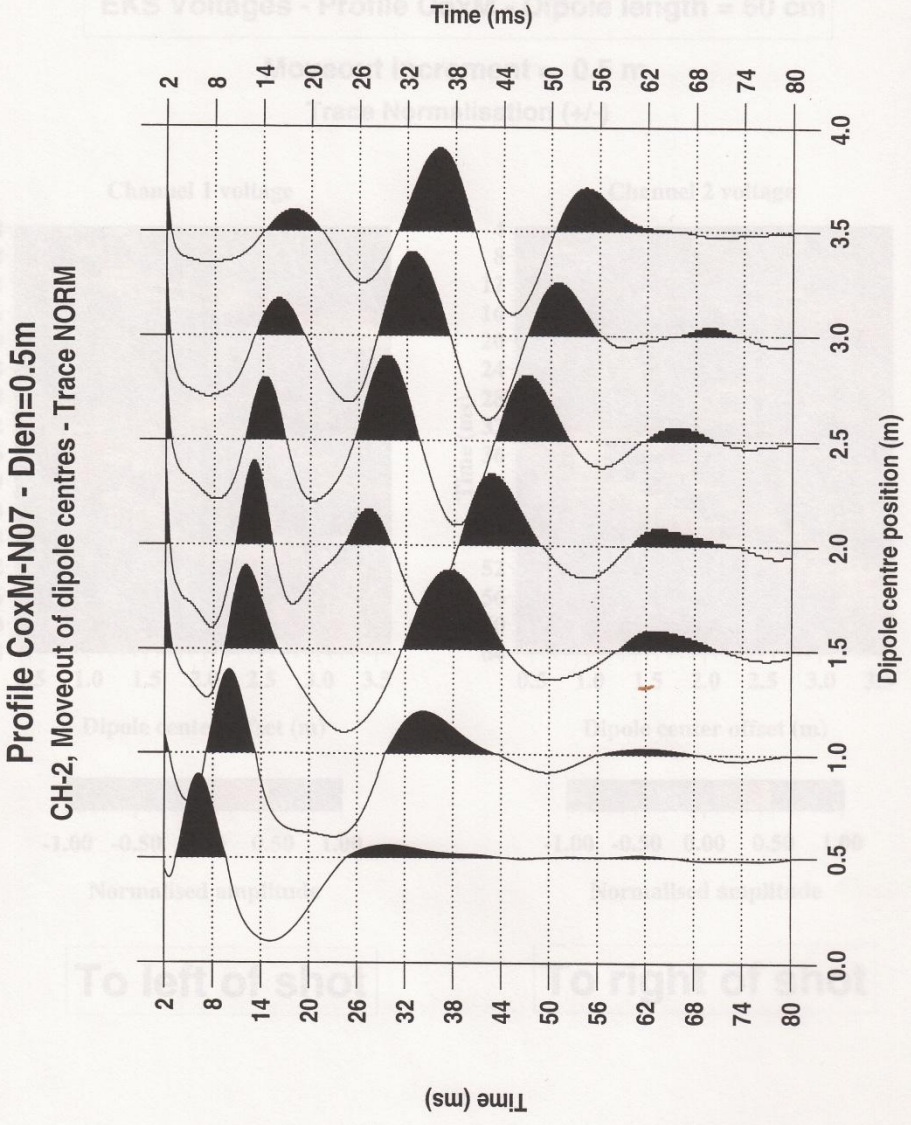

Fig. 6.4

Figure 6.4 Colour-contoured time/distance sections of voltage data

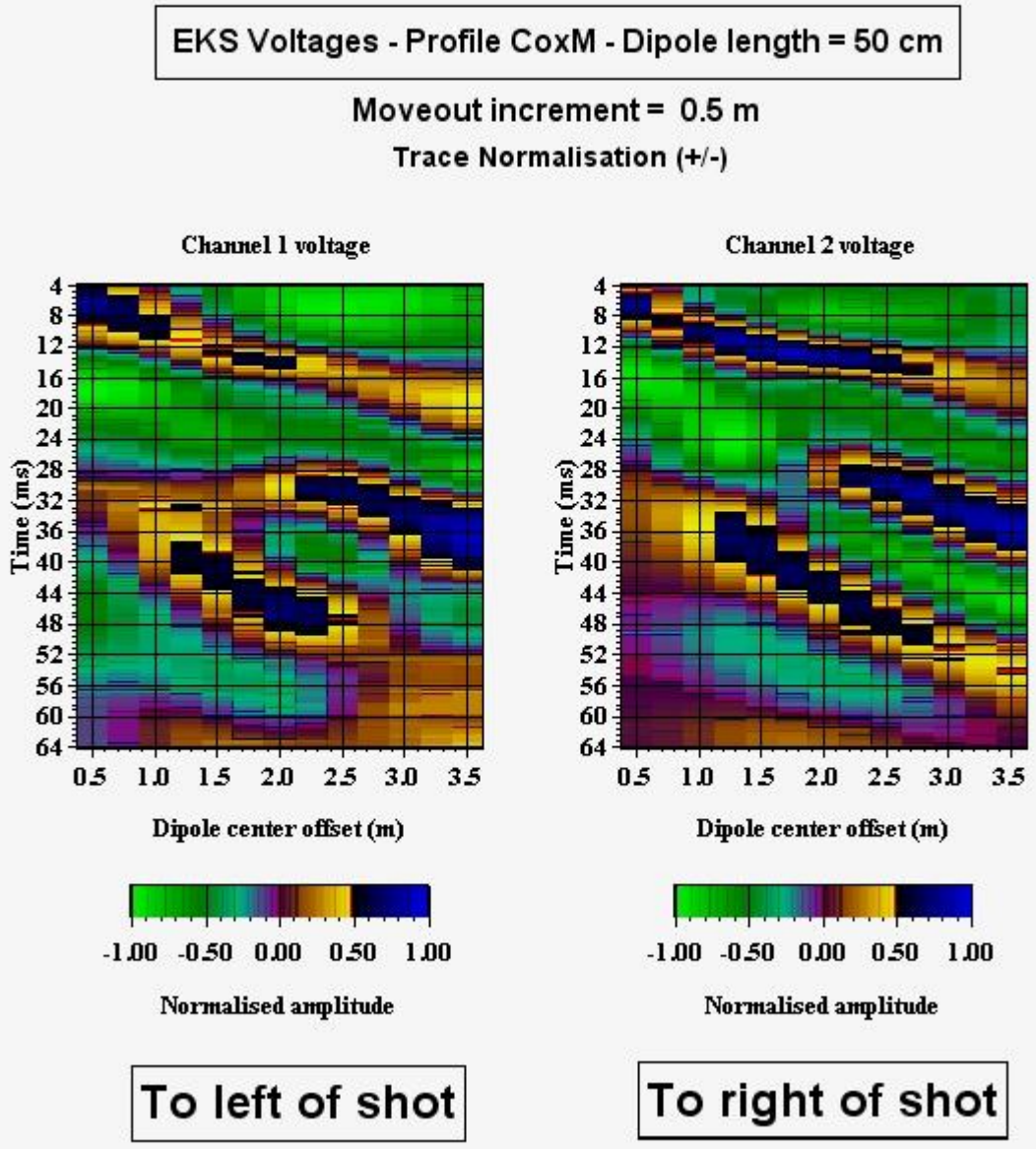

Fig. 6.5

Figure 6.5 Three soundings, same location, made with 3 electrode types (1=stainless steel), (2=Pb rods), (3=Cu/CuSO4)

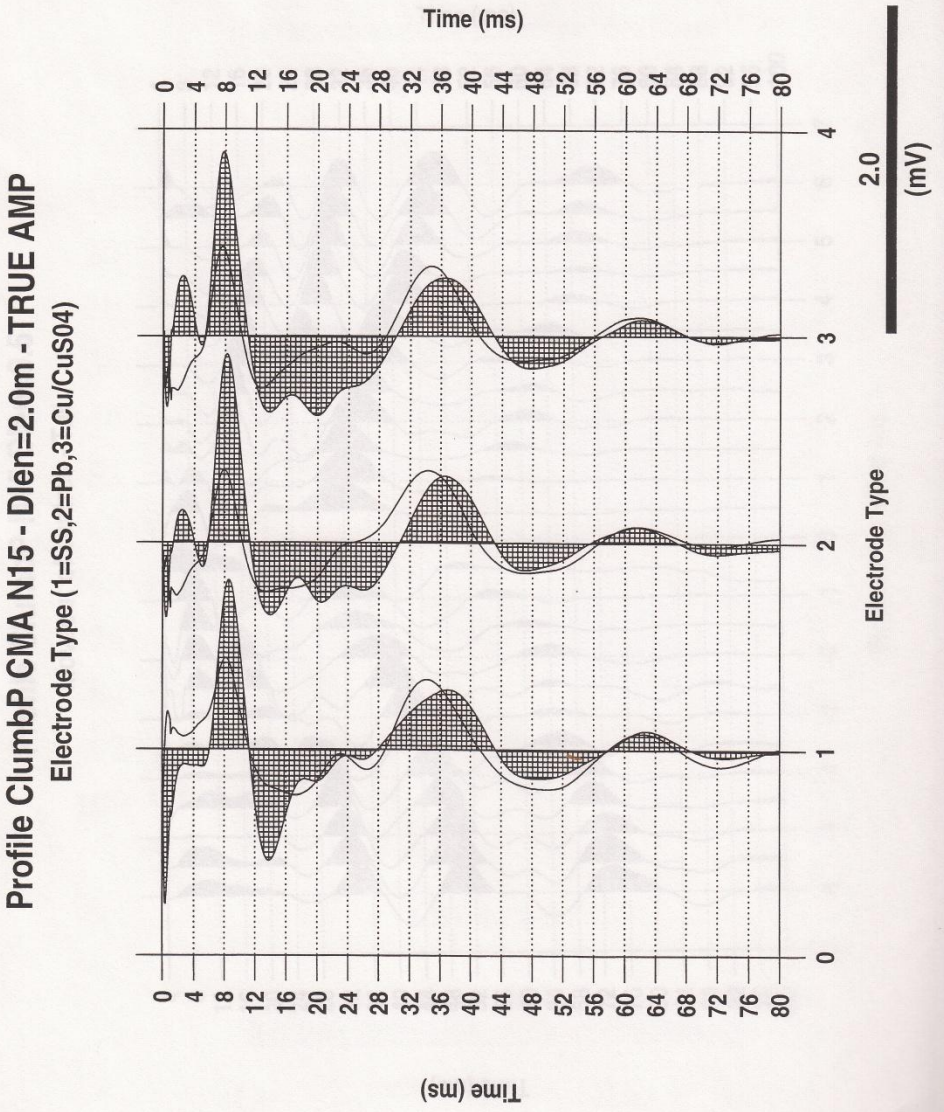

Fig. 6.6

Figure 6.6 Moveout experiment ClumbP-N15. Dipole length = 0.5 m. Trace normalised (+/-)

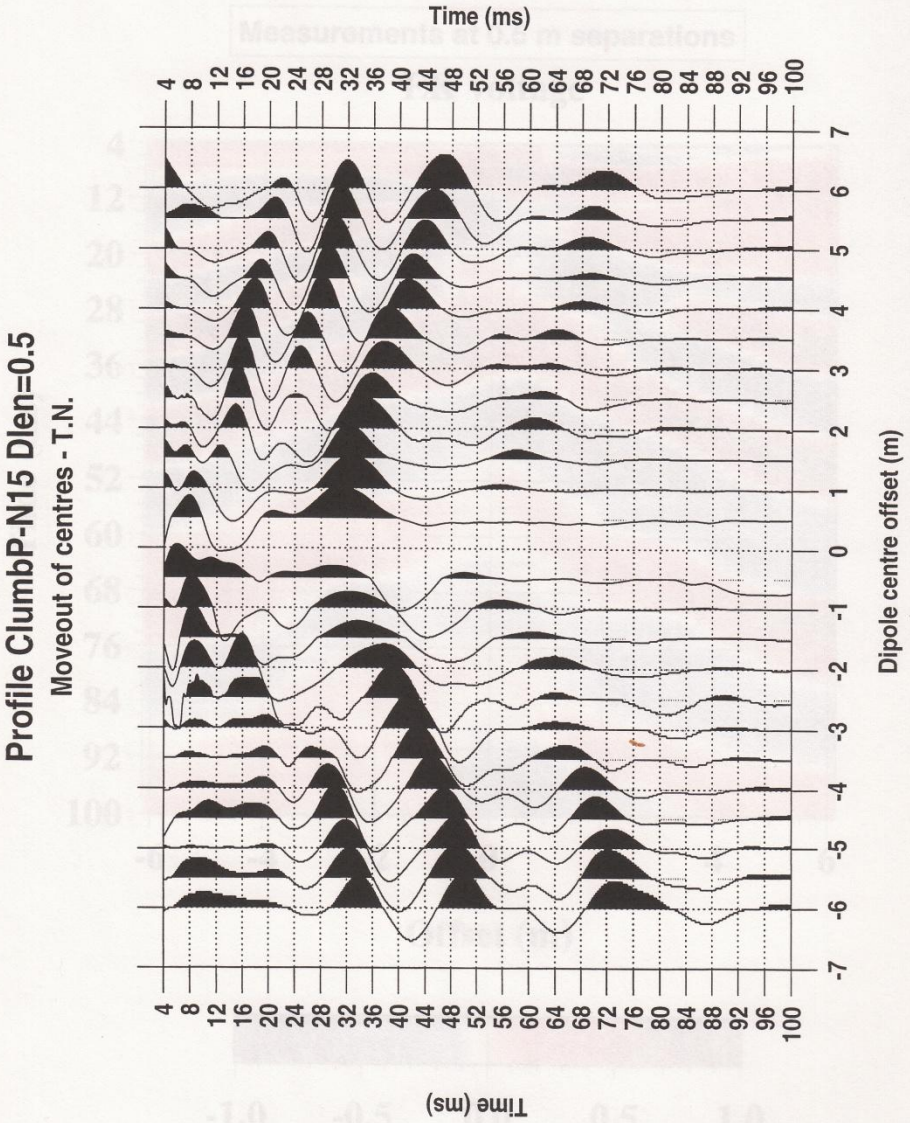

Fig. 6.7

Figure 6.7 Colour-contoured time/distance section of voltage data

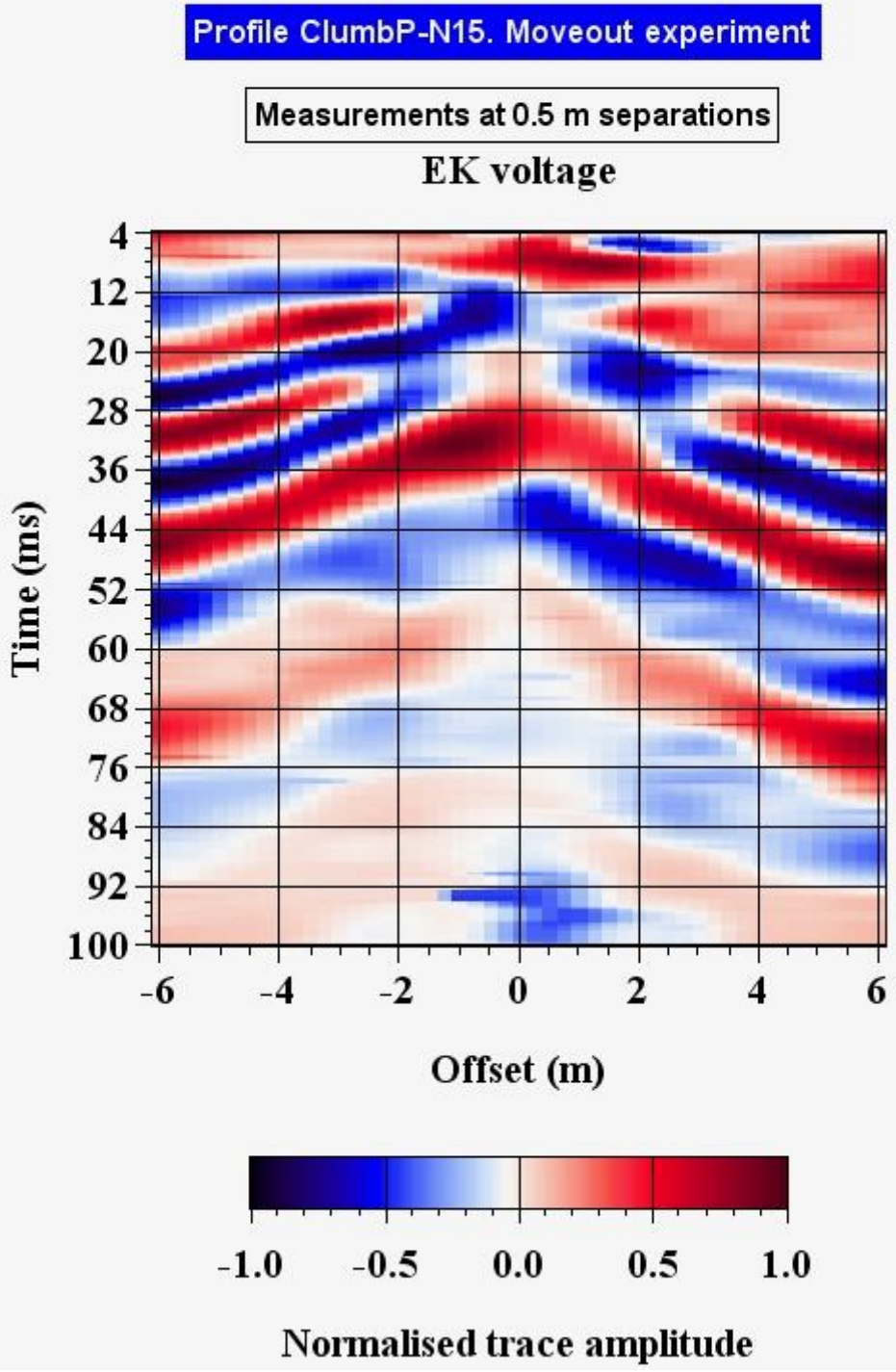

Fig. 6.8

Figure 6.8 Colour-contoured time/distance section of acoustic data

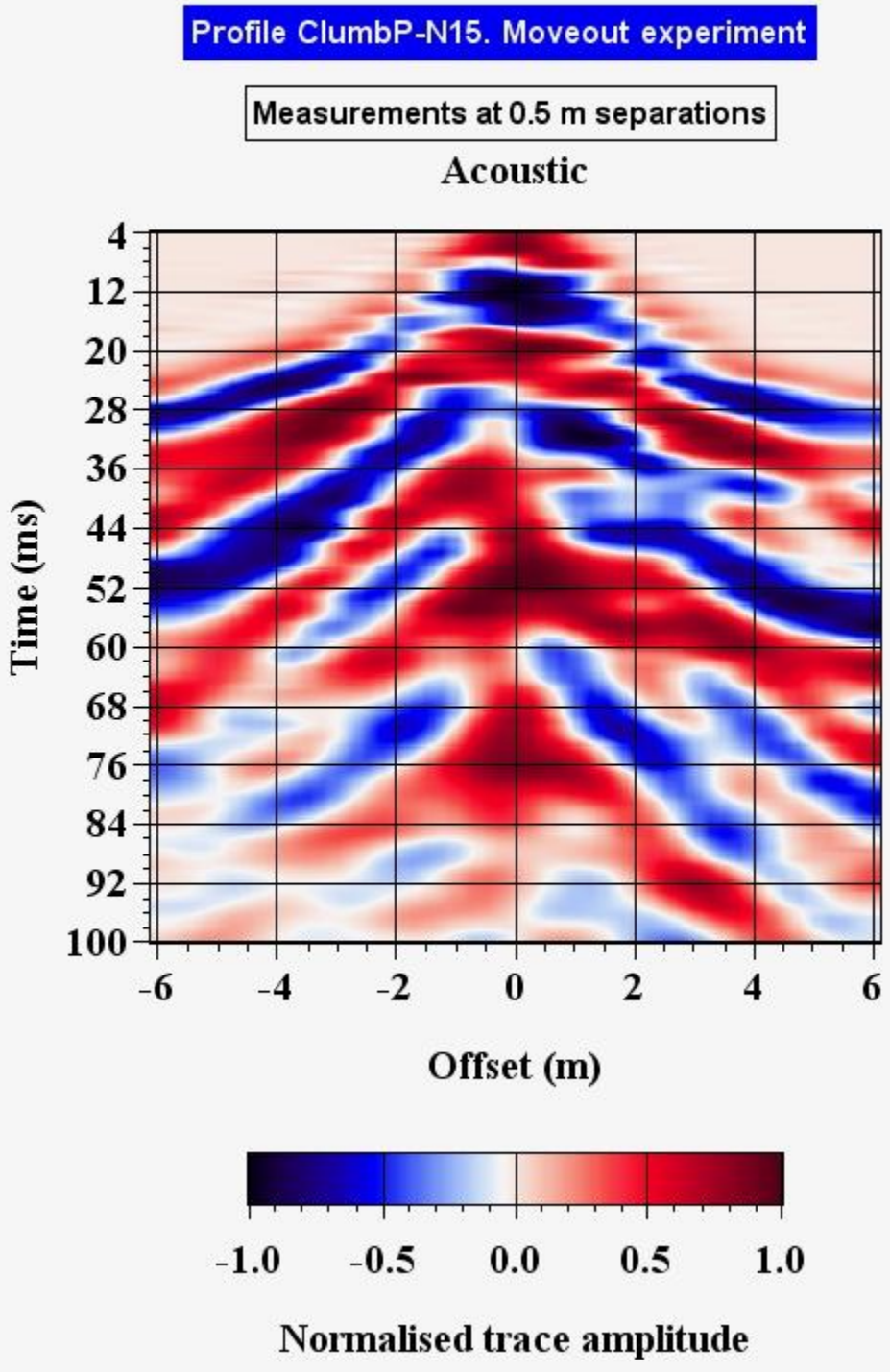

Fig. 6.9

Figure 6.9 Maximum Entropy power spectra of EK soundings with offsets varying from 1 to 5 m.

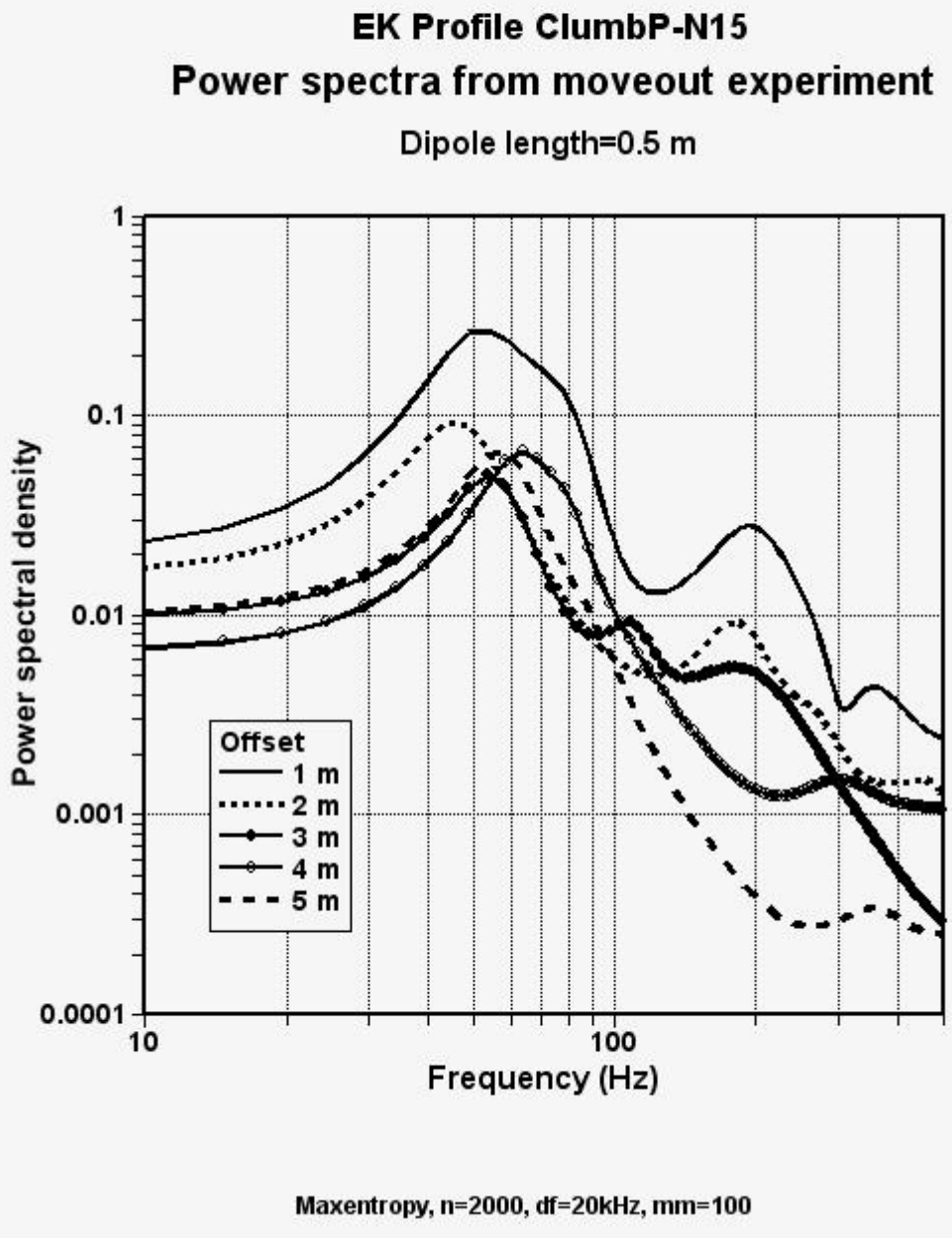

Fig. 6.10

Figure 6.10 Maximum Entropy power spectra of acoustic data with offsets varying from 1 to 5 m.

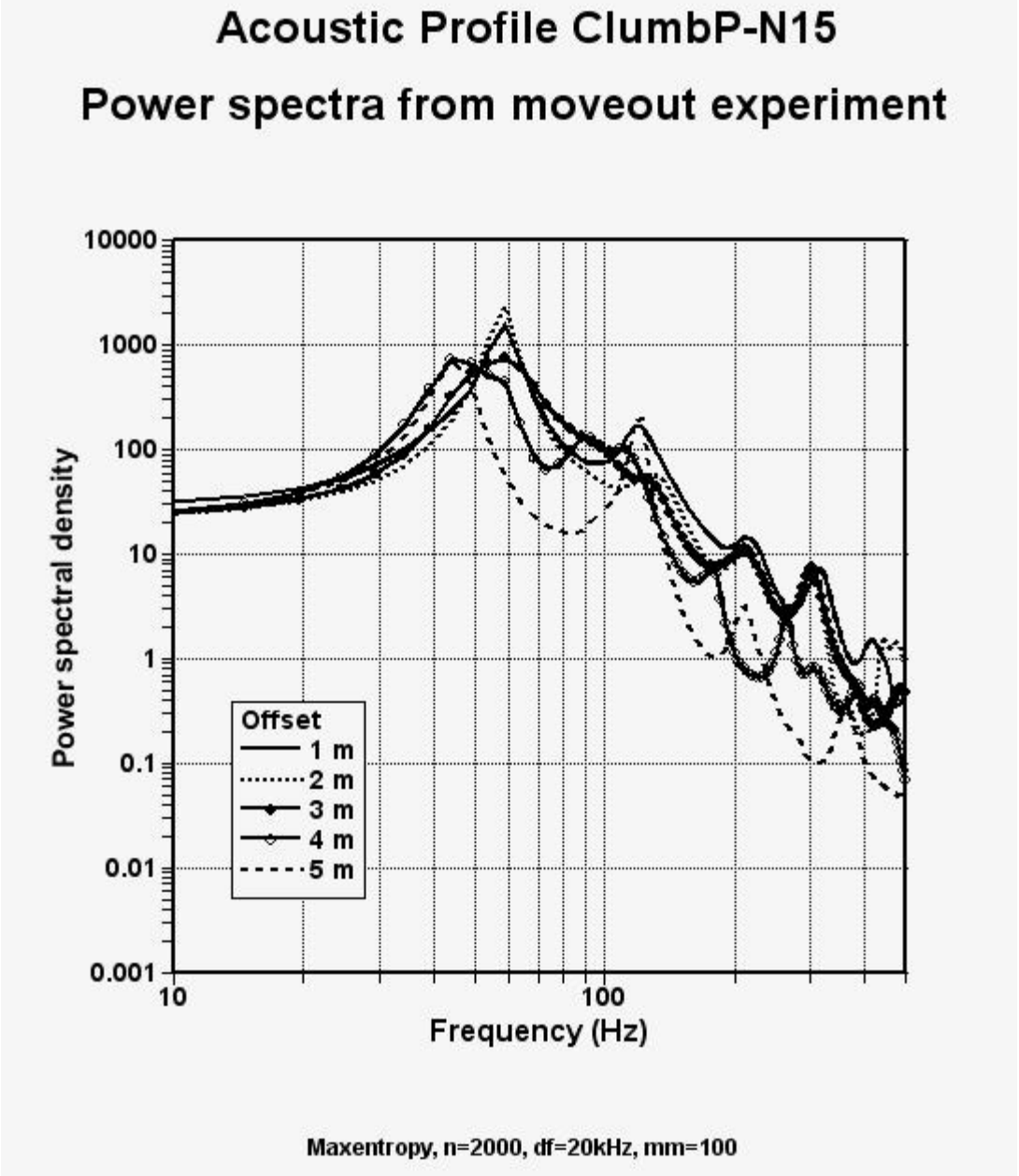

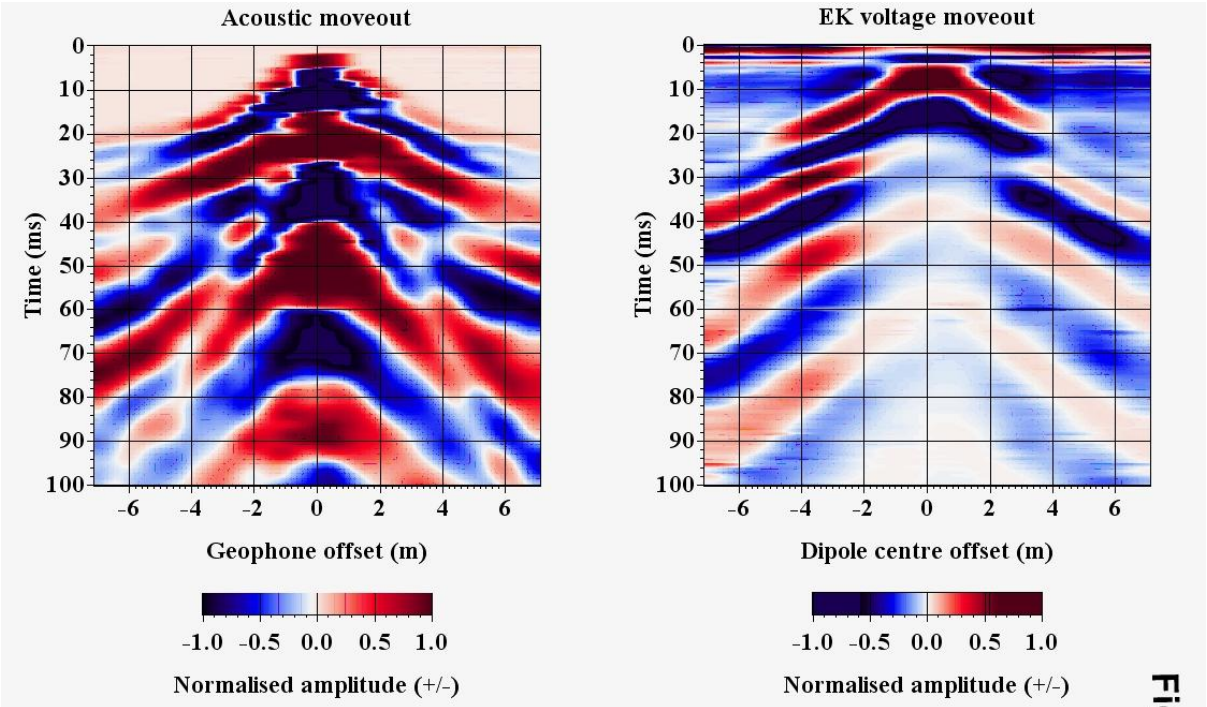

Figure 6.11 Detailed joint (acoustic and voltage) moveout experiment from the Gore sand river in Southern Zimbabwe. Sensor separations of 50 cm using 10 Hz geophones and 1 m dipoles. Data sampling of 20 kHz. Trace normalisation of + and - unity. The sand river is a drainage course incised in former pluvial periods and subsequently infilled with fine to coarse materials. The feature is some 15 m wide and 5 to 10 m deep.

Fig. 6.11

Fig. 6.12

Figure 6.12 EK sounding at 25 m along profile PA.
Postbridge survey, Dartmoor granite

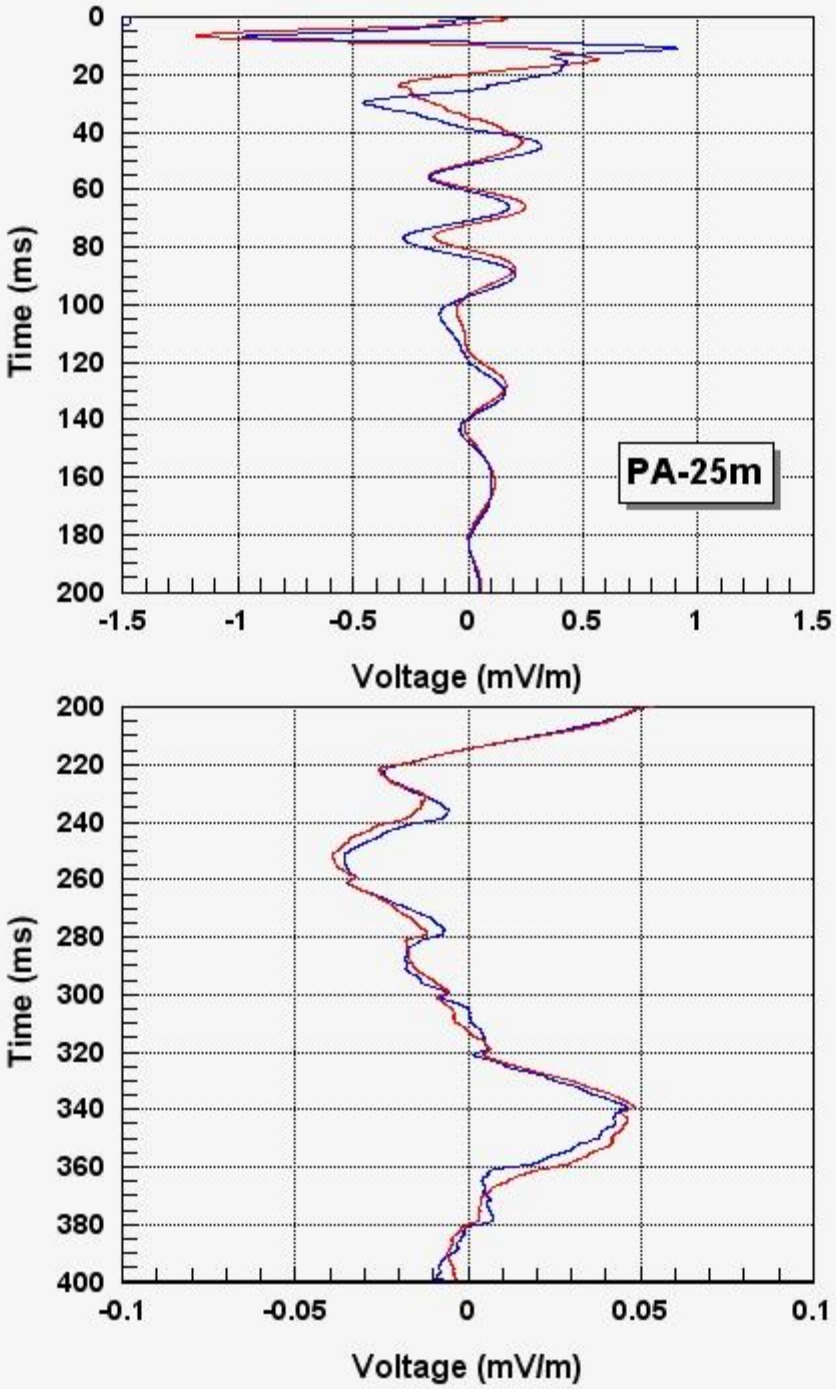

Fig. 6.13

Figure 6.13 EK sounding at 70 m along profile PA. Postbridge survey, Dartmoor granite

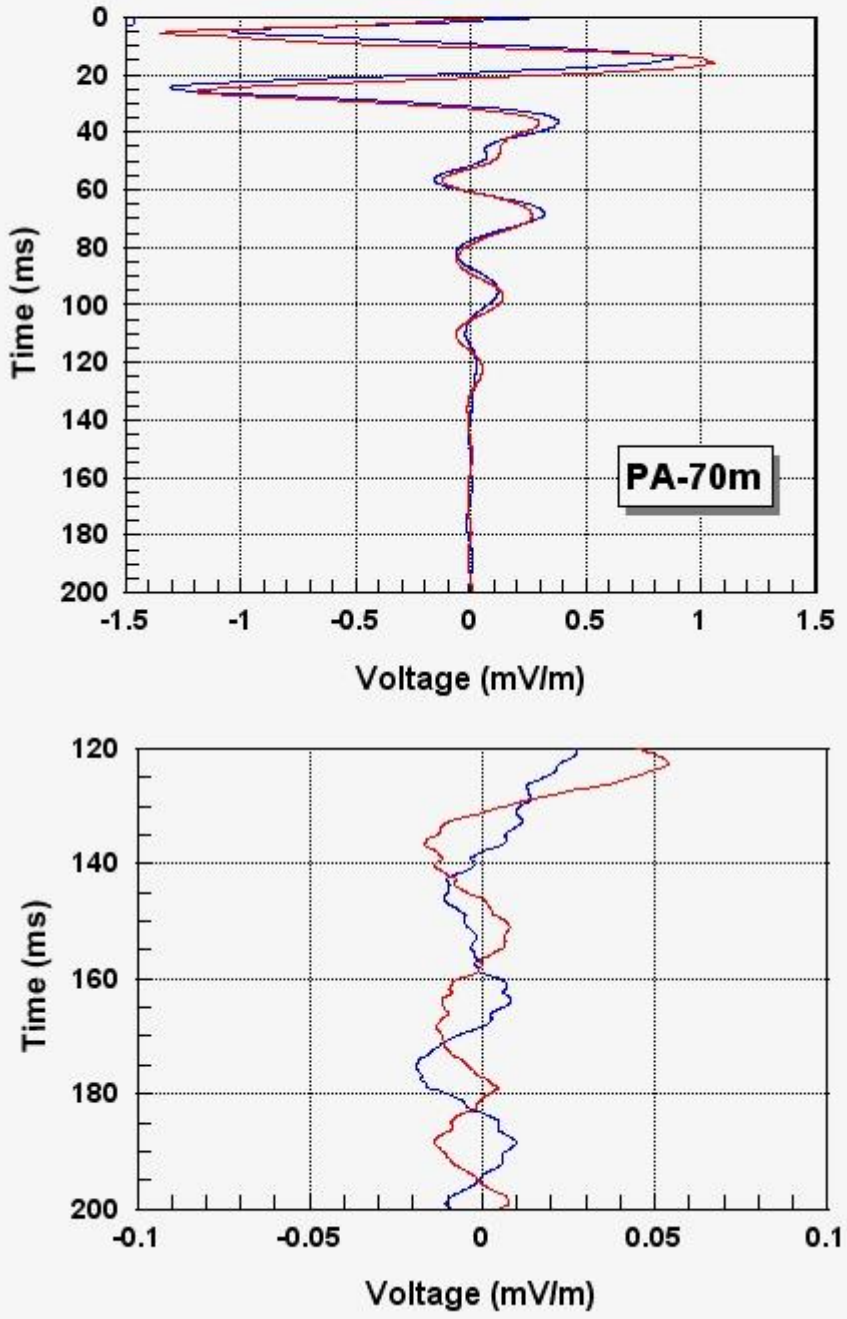

Fig. 6.14

Figure 6.14 Colour-contoured EK voltage data along profile. Channel 1 (upper), Channel 2 (lower)

Postbridge EK profile soundings, March 04

2m dipoles at 5m separations

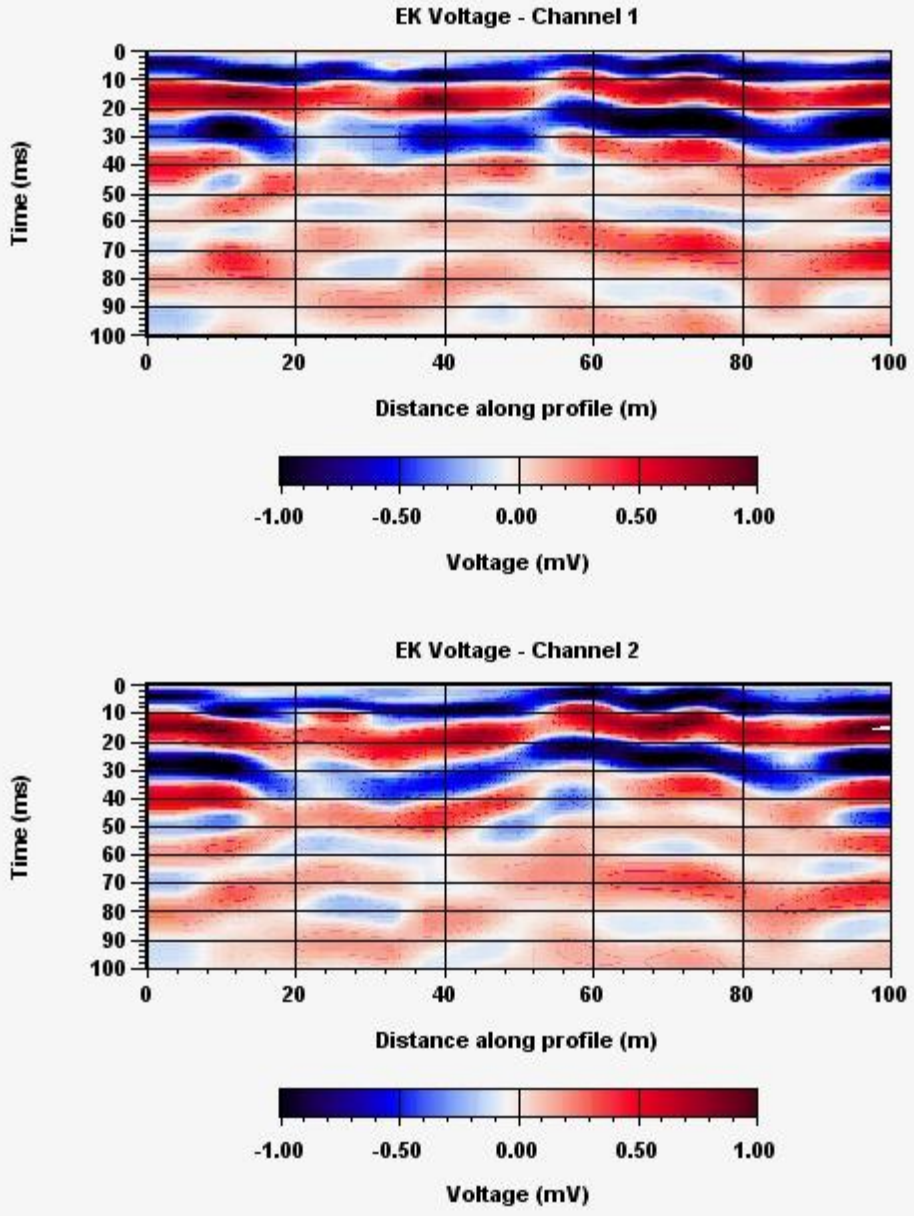

Fig. 6.15

Figure 6.15 Colour-contoured EK voltage data along profile. Channel 1 (upper), Channel 2 (lower)

Postbridge EK profile soundings, March 04

2m dipoles at 5m separations

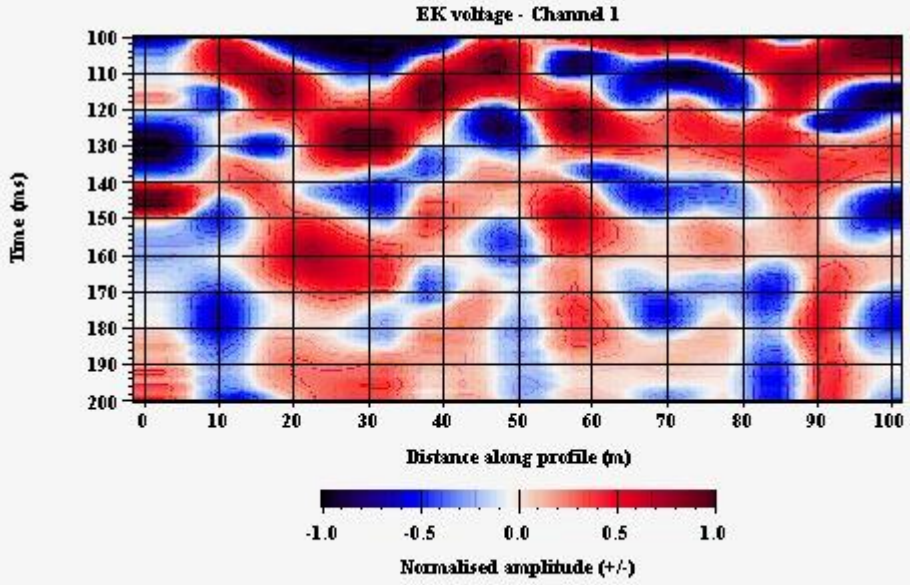

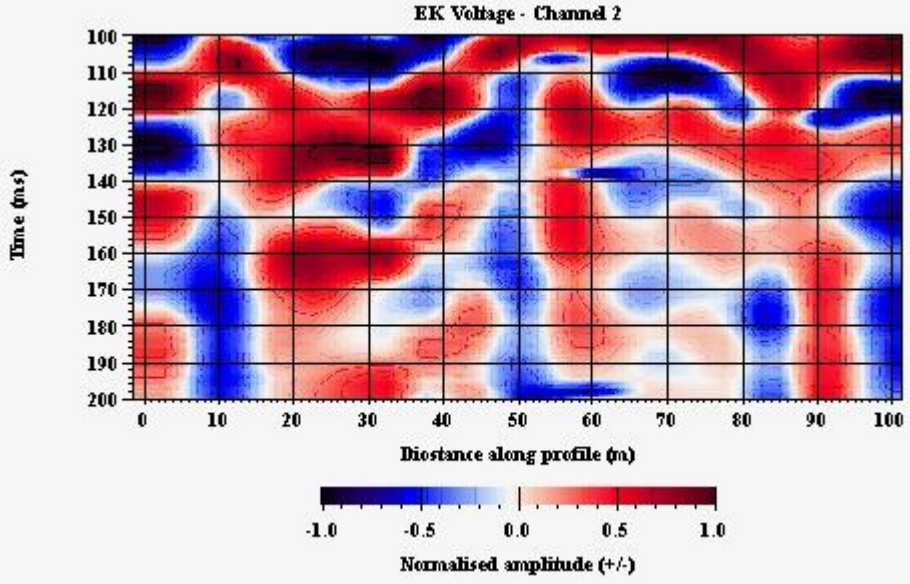

Additional Figures, not referred to in this report

Fig. 1

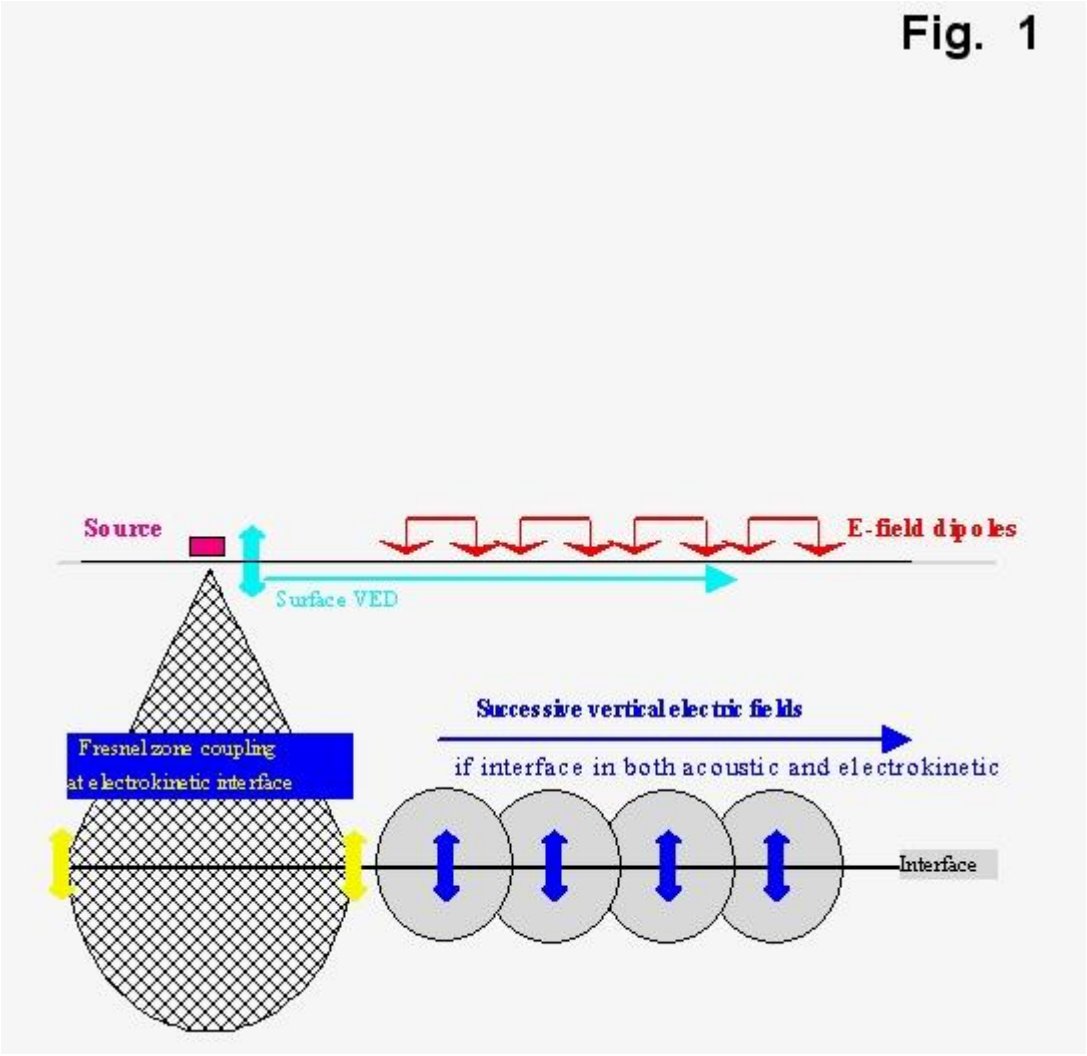

Fig. 2

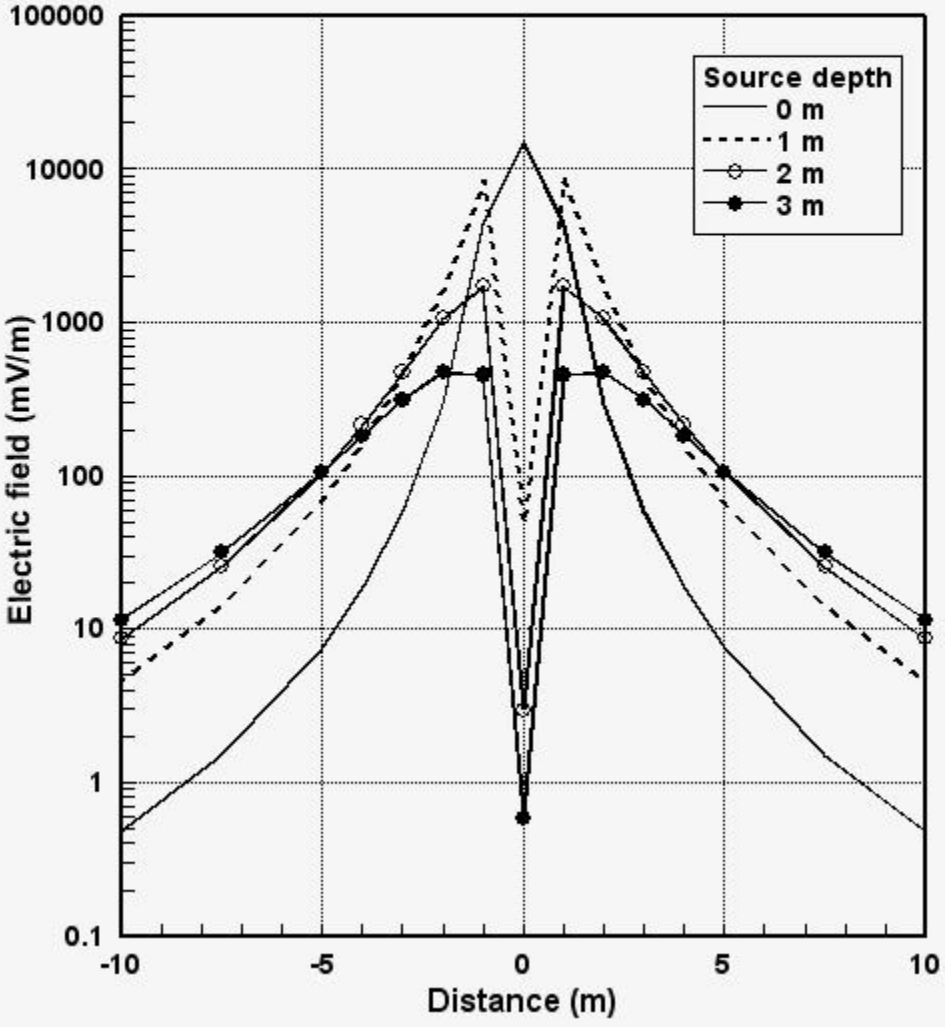
Source depth
0 m
1 m
2 m
3 m
Electric field (mV/m)
100000
10000
1000
100
10
1
0.1
-10
-5
0
5
10
Distance (m)

Fig. 3

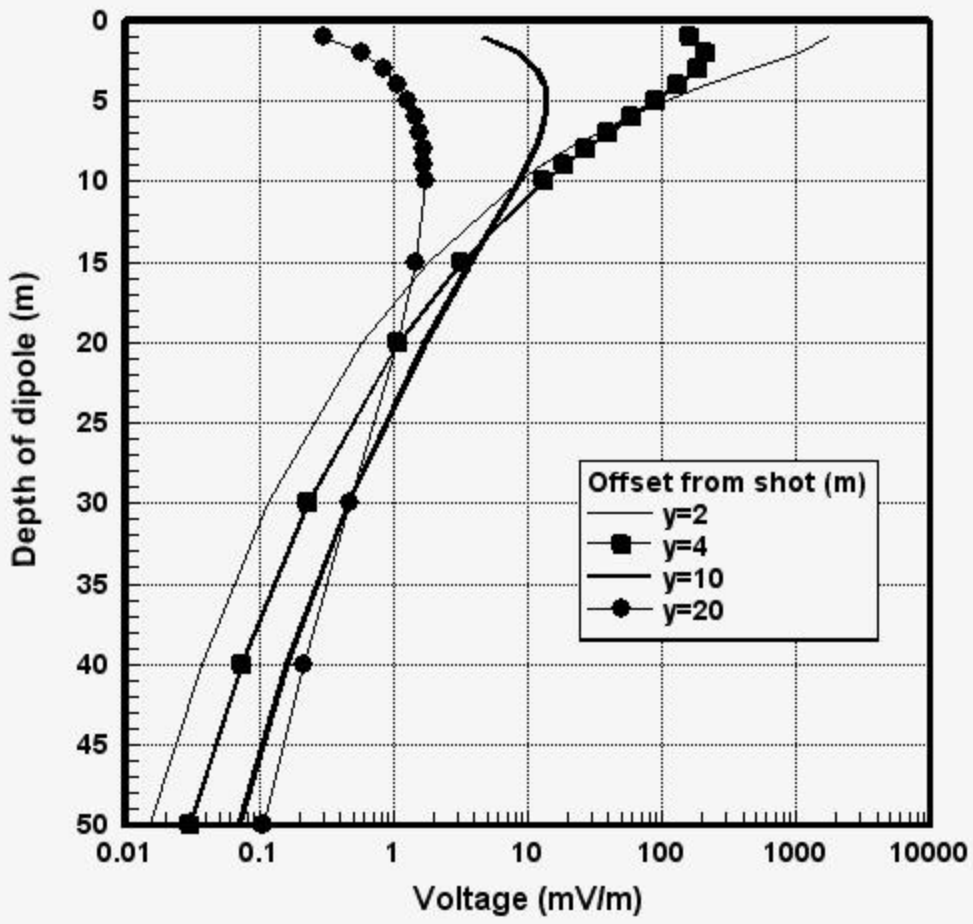
Depth of dipole (m)
0
5
10
15
20
25
30
35
40
45
50
0.01
0.1
1
10
100
1000
10000
Voltage (mV/m)
Offset from shot (m)
y=2
y=4
y=10
y=20

Fig. 4